Ubiquitin–proteasome-mediated cyclin C degradation promotes cell survival following nitrogen starvation

Stephen D. Willis[a], Sara E. Hanley[a], Thomas Beishke[a,†], Prasanna D. Tati[b], and Katrina F. Cooper[a,*]
[a]Department of Molecular Biology, Graduate School of Biomedical Sciences, and [b]School of Osteopathic Medicine, Rowan University, Stratford, NJ 08084

ABSTRACT **Environmental stress elicits well-orchestrated programs that either restore cellular homeostasis or induce cell death depending on the insult. Nutrient starvation triggers the autophagic pathway that requires the induction of several Autophagy (*ATG*) genes. Cyclin C–cyclin-dependent kinase (Cdk8) is a component of the RNA polymerase II Mediator complex that predominantly represses the transcription of stress-responsive genes in yeast. To relieve this repression following oxidative stress, cyclin C translocates to the mitochondria where it induces organelle fragmentation and promotes cell death prior to its destruction by the ubiquitin–proteasome system (UPS). Here we report that cyclin C-Cdk8, together with the Ume6-Rpd3 histone deacetylase complex, represses the essential autophagy gene *ATG8*. Similar to oxidative stress, cyclin C is destroyed by the UPS following nitrogen starvation. Removing this repression is important as deleting *CNC1* allows enhanced cell growth under mild starvation. However, unlike oxidative stress, cyclin C is destroyed prior to its cytoplasmic translocation. This is important as targeting cyclin C to the mitochondria induces both mitochondrial fragmentation and cell death following nitrogen starvation. These results indicate that cyclin C destruction pathways are fine tuned depending on the stress and that its terminal subcellular address influences the decision between initiating cell death or cell survival pathways.**

Monitoring Editor
Mark Solomon
Yale University

Received: Nov 13, 2019
Revised: Mar 2, 2020
Accepted: Mar 6, 2020

INTRODUCTION

In response to environmental cues, cells activate well-orchestrated processes to either restore cellular homeostasis or commit to cell death programs. Incorrectly deciding between these cell fates is detrimental to the cell and linked to the etiology of many diseases. The cellular response to adverse environmental cues can be divided into three stages. First, the stress damage is recognized and a signal transduced to the nucleus. Second, transcription programs are altered to repress progrowth programs while inducing genes necessary for detoxification and damage repair. Finally, the decision made in the nucleus has to be communicated to the organelles to provide a unified cellular response. Importantly, mitochondria are a key regulatory node for proper response to cellular damage with stress-induced fragmentation being an initial step in mitochondrion-dependent cell death pathways (Tait and Green, 2013; Kasahara and Scorrano, 2014).

The budding yeast *Saccharomyces cerevisiae* executes a regulated cell death (RCD) response to various stresses (oxidative stress, acetic acid, fungicides) (Madeo *et al.*, 1999; Ludovico *et al.*, 2002; Wissing *et al.*, 2004; Buttner *et al.*, 2007; Pereira *et al.*, 2007) that is coupled with a fragmented mitochondrial phenotype (Braun and Westermann, 2011; Cooper *et al.*, 2014). For example, although excessive hydrogen peroxide (H_2O_2) exposure initially induces both prosurvival (e.g., chaperones) and antioxidant (e.g., catalase) encoding genes (Levin, 2005), RCD inevitably ensues (Madeo *et al.*, 1999). In contrast, nitrogen limitation induces macroautophagy pathways (hereafter referred to as autophagy) that enhance recycling of

This article was published online ahead of print in MBoC in Press (http://www.molbiolcell.org/cgi/doi/10.1091/mbc.E19-11-0622) on March 11, 2020.
The authors declare no competing or financial interests.
†Present address: CooperSurgical, 5 Regent Street, Livingston, NJ 07039.
*Address correspondence to: Katrina F. Cooper (cooperka@rowan.edu).
Abbreviations used: Cdk, cyclin dependent kinase; CKM, Cdk8 kinase module; FACs, fluorescence activated cell; FDA, fluorescein diacetate; H_2O_2, hydrogen peroxide; HDAC, histone deacetylase; NPC, nuclear pore complex; OMM, outer mitochondrial membrane; RCD, regulated cell death; SRG, stress response genes; TORC, target of rapamycin complex; Ub, ubiquitin; UPS, ubiquitin–proteasome system.

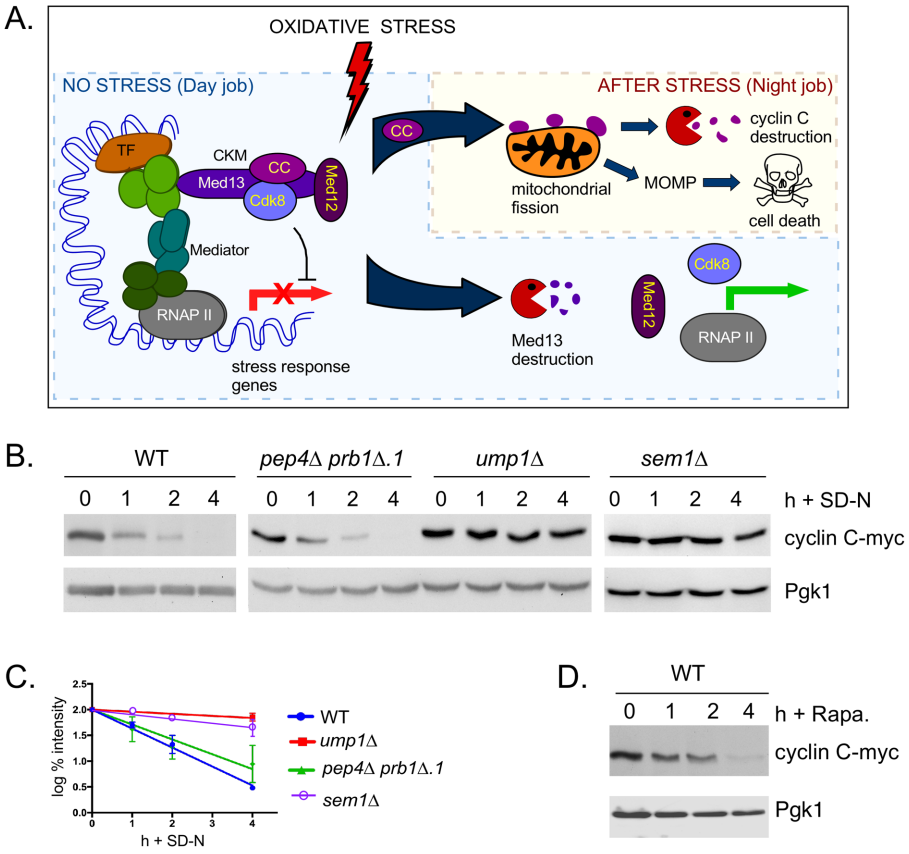

FIGURE 1: The UPS is required for cyclin C destruction following nitrogen starvation. (A) Model showing the two roles coined "day job" and "night job" that cyclin C plays to regulate the oxidative stress response (see text for details and reviewed in Jezek *et al.*, 2019b; Strich and Cooper, 2014). Importantly, the night job is independent of Cdk8 and both roles are conserved (Wang *et al.*, 2015). (B) Western blot analyses of extracts prepared from mid-log cultures with the indicated genotypes expressing cyclin C-myc resuspended nitrogen starvation medium (SD-N) for the indicated times. (C) Degradation kinetics of cyclin C signals obtained in B. Error bars indicate SD, $N = 3$. (D) Western blot analyses of extracts prepared from a wild-type mid-log culture were treated with 200 ng/ml rapamycin for the indicated times. Pgk1 levels were used as a loading control for all Western blot studies.

macromolecules and damaged organelles to maintain viability until nutrients become available (Krause and Gray, 2002; Galluzzi *et al.*, 2017). Autophagy requires induction of multiple autophagy-related (*ATG*) genes that either play general roles or execute specific assignments during specialized autophagic pathways (Cebollero and Reggiori, 2009). Most of the downstream effects, including autophagy upregulation, require inhibition of the conserved target of rapamycin complex 1 (TORC1) (Loewith and Hall, 2011; Conrad *et al.*, 2014). Moreover, amino acid or nitrogen starvation in mammalian cells induces a hyperfused mitochondrial network that promotes cell survival (Rambold *et al.*, 2011a; Gomes and Scorrano, 2013; Morita *et al.*, 2017). As a result, the mitochondria possess more cristae that optimize ATP production and promote survival.

Previous studies have shown that transcription of *ATG8*, a highly conserved gene required for phagophore formation during autophagy (Shpilka *et al.*, 2011), is repressed in nutrient-rich conditions by the Rpd3–Sin3–Ume6 histone deacetylase (HDAC) complex (Bartholomew *et al.*, 2012; Vlahakis *et al.*, 2017). Ume6 is a zinc cluster domain DNA-binding protein (Strich *et al.*, 1994) that tethers the Sin3–Rpd3 corepressor to promoters including *ATG8* (Kadosh and Struhl, 1997; Yukawa *et al.*, 2009; Vlahakis *et al.*, 2017). Its role in *ATG8* repression is consistent with the earlier findings that the Rpd3–Sin3–Ume6–Ume1 complex represses early meiotic genes whose transcription is also inhibited in nutrient-rich conditions (Vidal *et al.*, 1991; Strich *et al.*, 1994; Mallory and Strich, 2003). How repression is relieved upon nitrogen depletion is less well understood. For example, Rim15, the great wall kinase, induces *ATG8* transcription (Bartholomew *et al.*, 2012) but it remains unknown if this kinase works by inhibiting Ume6 or other HDAC members or by other mechanisms.

In addition to this HDAC complex, another repressor system was discovered that represses early meiotic genes (Strich *et al.*, 1989; Cooper *et al.*, 1997). This system is composed of the conserved Cdk8 kinase module (CKM) of the mediator complex (see Figure 1A). The CKM is composed of cyclin C, Cdk8, Med12, and Med13 and associates with the RNA polymerase II mediator complex and predominantly represses genes induced by environmental stress (Cooper *et al.*, 1997; Holstege *et al.*, 1998; Bjorklund and Gustafsson, 2005; van de Peppel *et al.*, 2005; Allen and Taatjes, 2015) and entry into meiosis (Cooper *et al.*, 1997; Strich *et al.*, 1989; Surosky *et al.*, 1994). In response to stress, cyclin C repression is relieved by its translocation to the cytoplasm (Cooper *et al.*, 2014) following the destruction of its nuclear anchor Med13 by the SCF^{Grr1} ubiquitin (Ub) ligase-mediated Ub–proteasome system (UPS) (Khakhina *et al.*, 2014; Stieg *et al.*, 2018). On translocation to the cytoplasm, cyclin C associates with mitochondria by directly binding to the fission machinery and inducing stress-mediated mitochondrial fragmentation (Cooper *et al.*, 2014; Strich and Cooper, 2014; Ganesan *et al.*, 2019; Jezek *et al.*, 2019b). In addition, cyclin C is required for promoting RCD (Krasley *et al.*, 2006; Cooper *et al.*, 2014). Finally, cyclin C is destroyed following mitochondrial fragmentation by the UPS (Cooper *et al.*, 1997, 2012), which attenuates the stress response. Taken together, these studies revealed that cyclin C connects the nuclear and mitochondrial oxidative stress response through its transcriptional repressor and mitochondrial morphology regulatory roles.

These studies are consistent with the emerging theme that proteins can have two very different functions, coined "day and night jobs" (Shamas-Din *et al.*, 2013; Gross and Katz, 2017), which can be induced by different external or intrinsic stimuli. Importantly, our studies have shown that both the day and night jobs of cyclin C are conserved (Wang *et al.*, 2015; Stieg *et al.*, 2019). More recently, we have shown that in mammalian cells, different domains of cyclin C directly interact with the mitochondrial fission GTPase Drp1 to direct stress-induced mitochondrial fission (Ganesan *et al.*, 2019). The cyclin C–Bax interaction is required for normal Bax activation and its efficient mitochondrial localization (Jezek *et al.*, 2019a). Further studies in both yeast and mammals revealed that the aberrant release of cyclin C does not kill cells but does make them hypersensitive to oxidative or chemotherapeutic damage

(Khakhina *et al.*, 2014; Jezek *et al.*, 2019a). Taken together, these results demonstrate that cyclin C translocation to the mitochondria is an early step in the RCD pathway (Jezek *et al.*, 2019a). As anticipated from these results, both yeast and mammalian cells devoid of cyclin C are less sensitive to stress (Cooper *et al.*, 2014; Wang *et al.*, 2015) and acts as a tumor suppressor in both solid and hematological cancers (Li *et al.*, 2014; Jezek *et al.*, 2019c).

Given cyclin C's bipartite role following cell death stimuli, we investigated whether it has a regulatory role when cells induce the autophagic survival response following nitrogen starvation. Similar to oxidative stress, we discovered that cyclin C represses the transcription of a gene (*ATG8*) required for autophagy. In addition, genetic studies revealed that cyclin C-Cdk8 function in the same pathway as the Ume6-Rpd3 HDAC system. Cyclin C–Cdk8-dependent repression in nitrogen-starved cells is also relieved by cyclin C proteolysis via the UPS. However, several differences from oxidatively stressed cells were observed. First, no detectable cytoplasmic cyclin C was seen and the mitochondria remained reticular. This difference is important as targeting cyclin C to the mitochondria changed nitrogen starvation from evoking a survival pathway to one inducing cell death. These findings reveal a complex system in which the subcellular address of cyclin C plays a key role in cell fate decisions by regulating gene expression and mitochondrial-dependent RCD.

RESULTS

Cyclin C degradation following nitrogen starvation requires 26S proteasome activity

We previously reported that cyclin C relocalization and subsequent destruction play key roles in directing cell fate following oxidative stress (Cooper *et al.*, 2012, 2014; Jin *et al.*, 2014a). Therefore, we asked whether cyclin C is similarly regulated upon nitrogen starvation. Exponentially growing wild-type cells expressing a functional cyclin C-myc reporter (Cooper *et al.*, 1997) were starved for nitrogen (SD-N) and cyclin C levels were monitored by Western blot analysis. The results showed that cyclin C levels were reduced following nitrogen starvation with an apparent half-life of 45 min (Figure 1B, quantified in Figure 1C, half-life in Supplemental Figure S1A). Rapamycin also inhibits TORC1 (Cardenas *et al.*, 1999) by a mechanism not physiologically identical to nitrogen starvation (Tate and Cooper, 2013). Therefore, we repeated these experiments in replete medium containing rapamycin at 200 ng/ml. Western blot analysis produced results similar to those obtained with nitrogen starvation (Figure 1D, quantified in Supplemental Figure S1A) with the decay rate being slightly slower (half-life of 75 min). The same rate of decay was also obtained when 50 ng/ml rapamycin was used (Supplemental Figure S1, A and B). Treatment with rapamycin, but not it's solvent (Tween/ethanol), also triggered cyclin C destruction when tagged with YFP (Supplemental Figure S1C). We previously demonstrated that *CNC1* mRNA levels remain constant following 4 h nitrogen starvation (Cooper *et al.*, 1999) and found that the half-life of cyclin C is ~3 h in unstressed cultures using cycloheximide translation inhibition assays (Supplemental Figure S1, D and E). Taken together, these results suggest that cyclin C is targeted for degradation following nitrogen starvation or rapamycin stress. Next, we addressed whether cyclin C destruction required either the vacuolar or the UPS pathways. First, cyclin C-myc levels were monitored in nitrogen-starved cultures harboring mutations in two major vacuolar proteases, Pep4 and Prb1 (Takeshige *et al.*, 1992; Van Den Hazel *et al.*, 1996). The results showed that cyclin C was degraded with similar kinetics to wild type (Figure 1B, quantified in Figure 1C). In contrast, repeating this experiment in a mutant deficient for normal 20S proteasome assembly (*ump1*Δ) (Ramos *et al.*, 1998; Li *et al.*, 2007; Czabotar *et al.*, 2013; Uekusa *et al.*, 2014), significantly stabilized cyclin C (Figure 1B, quantified in Figure 1C). These results indicate that the UPS degrades cyclin C in response to nitrogen starvation.

Cyclin C degradation following nitrogen starvation requires 19S proteasome activity

It has been reported that the 20S proteasome can degrade ubiquitylated proteins independent of 19S function (Wang *et al.*, 2010). To address if 19S function is required for cyclin C degradation in response to nitrogen starvation, a *sem1*Δ mutant was used. Sem1 is required for efficient lid assembly, catalyzing the incorporation of subunits Rpn3 and Rpn7 into the 19S regulatory complex (Jantti *et al.*, 1999; Tomko and Hochstrasser, 2014). Cyclin C was significantly stabilized in *sem1*Δ compared to wild-type cells (Figure 1B, quantified in Figure 1C). Taken together, these results confirm the above conclusions that the UPS is required for cyclin C degradation and that the cap region is required for this activity.

Cyclin C destruction following nitrogen starvation uses the same E2s but different E3 enzymes to oxidative stress

UPS-mediated destruction is executed by proteins being tagged with Ub chains by a sophisticated three-step enzymatic cascade utilizing E1 Ub-activating, E2 Ub–conjugating and a variety of E3 Ub-ligating enzymes (Pickart, 2001; Tsuchiya *et al.*, 2017). Ub chains are in turn recognized by intrinsic or extrinsic (or a combination of both) receptor proteins that deliver and/or capture tagged proteins to the 19S cap of the proteasome (Schauber *et al.*, 1998; Hartmann-Petersen *et al.*, 2003; Verma *et al.*, 2004; Lander *et al.*, 2012; Rosenzweig *et al.*, 2012; Shi *et al.*, 2016). As H_2O_2-mediated destruction of cyclin C requires the action of the functionally redundant *UBC4 and UBC5* E2 enzymes (Cooper *et al.*, 1999, 2012), we investigated whether they performed the same role in nitrogen-starved cells. Cyclin C was significantly stabilized in *ubc4*Δ *ubc5*Δ cells compared with the isogenic wild type under these conditions (Figure 2A, quantified in Figure 2B). Next, the role of Ub receptor proteins in cyclin C proteolysis was tested. Cyclin C was still subjected to at least partial proteolysis in strains harboring single, double, and triple deletions in the extrinsic receptor proteins Ddi1, Dsk2, and Rad23 (Supplemental Figure S2A). Likewise, partial proteolysis was observed in strains harboring single and double deletions in Rpn10 and Rpn13, the intrinsic receptor proteins (Supplemental Figure S2B). Intriguingly, compared with its isogenic wild type, partial proteolysis of cyclin C was also observed in the intrinsic receptor triple mutant strain (Figure 2C) in which Rpn1, Rpn10, and Rpn13 each harbor mutations that prevent Ub binding (Shi *et al.*, 2016). However, cyclin C was significantly stabilized in the "*quint*Δ" receptor mutant strain (Figure 2C, quantified in Figure 2B), in which the only functional Ub receptor is Rpn1 (Shi *et al.*, 2016). Therefore, similar to other UPS substrates (Zhang *et al.*, 2009; Shi *et al.*, 2016; Saeki, 2017), the extrinsic and intrinsic Ub receptors are functionally redundant with regard to cyclin C degradation following nitrogen starvation. A caveat to this interpretation is that Sem1 is a potential Ub receptor, having such a role in fission yeast. However, here Sem1 does not recognize Ub when assembled in the complete proteasome (Paraskevopoulos *et al.*, 2014).

We next asked if Not4, the E3 ligase that mediates cyclin C destruction following oxidative stress (Cooper *et al.*, 2012, 2014), also plays this role in nitrogen-starved cells. However, cyclin C was still destroyed after 4 h nitrogen depletion in *not4*Δ cells (Figure 2E) indicating that a different E3 ligase fulfills this role. As Ubc4/5 can interact with both HECT domain and RING E3 ligases (Stoll *et al.*, 2011), we decided to hunt for the E3 ligase mediating cyclin C degradation

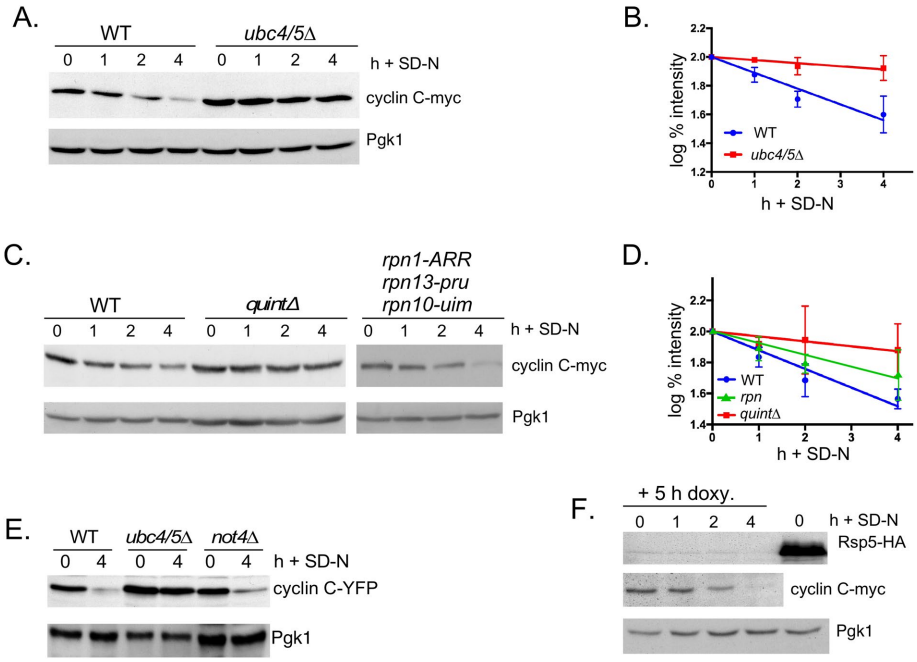

FIGURE 2: The UPS is required for cyclin C degradation following nitrogen starvation. (A) Western blot analyses of extracts prepared from mid-log *ubc4/5*Δ (MHY508) and wild-type (MHY414) cultures expressing cyclin C-myc resuspended in nitrogen starvation medium (SD-N) for the indicated times. (B) Quantification of the results obtained in A. $N = 3$. (C) As in A except that cyclin C levels were monitored in wild type (SUB62), the "*quint*Δ" Ub receptor mutant (YSS781a, *dsk2*Δ, *rad23*Δ, *ddi1*Δ *rpn13-pru rpn10-uim)*, and the triple intrinsic receptor mutant (YSS786a, *rpn13-pru rpn10-uim rpn1-ARR*). (D) Quantification of the results obtained in C. $N = 2$. (E) Cyclin C-YFP was monitored by Western blot analysis following nitrogen starvation in wild type (MHY414), *ubc4/5*Δ (MHY508), and *not4*Δ. (F) The Rsp5-HA strain (RSY2301) harboring the Tet operator plasmid (pCM1888) and cyclin C-myc were grown to mid-log phase and a sample removed for Western analysis to visualize Rsp5-HA (far right, top panel). The remaining culture was treated with doxycycline for 5 h before being subjected to nitrogen starvation. Thereafter, cyclin C-myc was monitored by Western blot analysis. For all blots, Pgk1 levels were used as loading controls.

by initially testing candidate genes. Rsp5 was first tested as it both interacts with RNA polymerase II and is involved in a variety of stress responses (Huibregtse *et al.*, 1997; Wang *et al.*, 1999; Hiraishi *et al.*, 2009). A doxycycline-inducible N-end rule approach (Bachmair *et al.*, 1986; Varshavsky, 1992; Gnanasundram and Kos, 2015) was used as Rsp5 is an essential gene and cyclin C is rapidly degraded in response to heat shock (Cooper *et al.*, 1997) forbidding the use of temperature-sensitive alleles. The administration of doxycycline depleted the Rsp5-HA N-end rule degron from yeast cells (Figure 2F, top panel,) but cyclin C was still degraded following nitrogen starvation in these cells (Figure 2F, middle panel). Cyclin C was also degraded in the other candidate HECT domain E3 ligases that reside in the nucleus (Hul5, Rsp5, Tom1, Ufd4) (Finley *et al.*, 2012) as well as in *ars1*Δ (Supplemental Figure S2, C and D). This latter E3 was considered a good candidate as it directly binds Rpb1, a subunit of RNA polymerase II (Daulny *et al.*, 2008). We subsequently screened deletion mutants of viable putative single E3 ligases identified to date (see Supplemental Table S1 and Finley *et al.*, 2012; Zhu *et al.*, 2016) but did not find any single mutant that blocked cyclin C degradation (see Supplemental Figure S2E for a representative Western blot and *Materials and Methods* for details). Likewise, cyclin C was destroyed in nitrogen-starved cells harboring N-end rule degron alleles of the two remaining essential ligases (Skp1 of the SCF and Tfb3; Supplemental Figure S2, F and G). Taken together, these results suggest that similar to other substrates (Zhang *et al.*, 2009; Shi *et al.*, 2016; Saeki, 2017), multiple Ub ligases mediate cyclin C proteolysis during nitrogen starvation.

Cyclin C does not translocate to the mitochondria following nitrogen starvation

Cyclin C is nuclear during normal growth conditions but forms mitochondrial-associated foci required for organelle fragmentation in response to oxidative stress (Cooper *et al.*, 2014; Jin *et al.*, 2014a) (see Figure 3A, top and middle panels). Thereafter cyclin C is destroyed by the UPS in the cytoplasm (Cooper *et al.*, 1997, 2012). To determine whether cyclin C responds similarly following TORC1 inhibition, subcellular localization of cyclin C-YFP and mitochondrial morphology were monitored by fluorescence microscopy following 200 ng/ml rapamycin treatment. These experiments revealed that cyclin C-YFP was below the limits of detection following rapamycin treatment using standard exposure times (Figure 3A, bottom panel). No observable cyclin C-YFP cytoplasmic presence was observed even when longer exposures were used in cells harboring an NLS-NAB-mCherry fusion protein (Malinovska *et al.*, 2012) to mark the nucleus (Supplemental Figure S3, A and B). Likewise, no observable cyclin C-YFP cytoplasmic presence was observed even at earlier timepoints in cells harboring a Nup49-mCherry fusion protein that marks the nuclear pore complex (NPC; Bucci and Wente, 1997) (Figure 3B). Last, consistent with the model that vacuolar hydrolysis is not needed to degrade cyclin C, we did not observe cyclin C-YFP in vacuoles marked by Vph1-mCherry in WT (Figure 3C) or *pep4*Δ *prb1*Δ*-1* strains (Figure 3D). Likewise, cyclin C-YFP was still detectable in *ump1*Δ cells after rapamycin treatment with the caveat that we also observed some unexplained foci that were predominantly nuclear in both unstressed and stressed cells (Supplemental Figure S3D).

Consistent with cyclin C not having an observable cytoplasmic presence, we observed that the mitochondria remain predominantly reticular following 200 ng/ml rapamycin stress (Figure 3, A and C). These findings match early reports in mammalian cells that mitochondrial fragmentation is infrequent during starvation (Gomes *et al.*, 2011; Rambold *et al.*, 2011a,b). As nitrogen starvation triggers a slightly different stress response (Tate and Cooper, 2013), we next examined cyclin C-YFP localization and mitochondrial morphology during nitrogen depletion. Figure 4A shows that identical to rapamycin treatment, cyclin C-YFP was below the limits of detection after 3 h in nitrogen starvation media. Furthermore, these cells also harbored Nup49-mCherry and no observable cytoplasmic presence was detected at earlier timepoints (1 and 2 h). Importantly, even after longer exposure times (4 h) to nitrogen starvation media, the mitochondria remained predominantly reticular (Figure 4B) and cyclin C was only detectable on overexposure (Supplemental Figure S3D). Taken together, these data indicate that similar to oxidative stress, cyclin C is destroyed by the UPS following TORC1

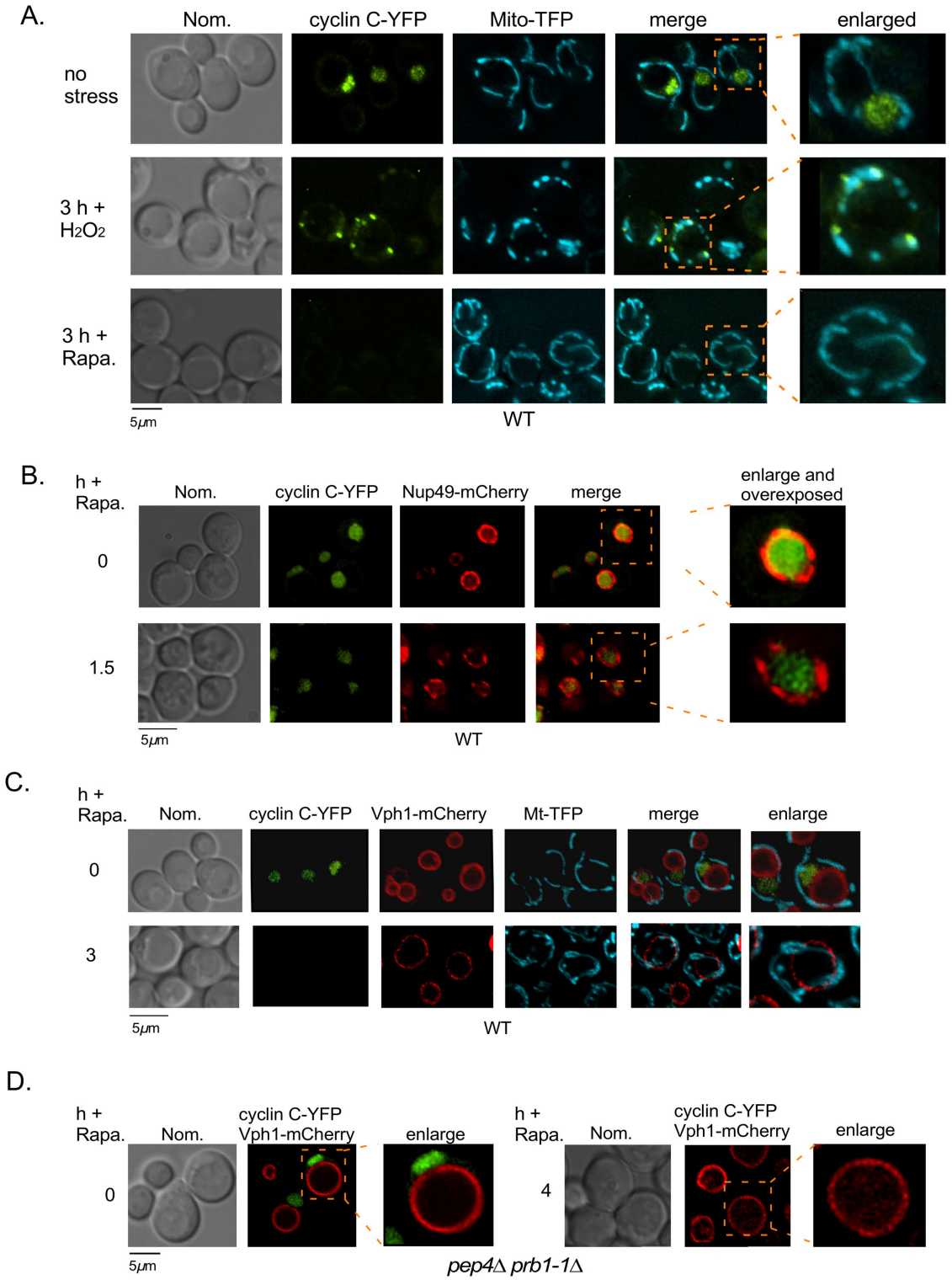

FIGURE 3: Cyclin C does not induce mitochondrial fragmentation following rapamycin stress. (A) Wild-type cells (RSY10) harboring expression plasmids for Mito-TFP (mitochondrial marker) and cyclin C-YFP were untreated (top panels) treated with 0.8 mM H_2O_2 (middle panel) or rapamycin (200 ng/ml) for the times indicated. Merged panels of cyclin C-YFP and Mito-TFP are shown. The stippled box indicates enlarged panels. (B) Wild-type cells harboring cyclin C-YFP and Nup49-mCherry grown to mid-log were treated with rapamycin (200 ng/ml) as indicated. Merged and enlarged panels are indicated. (C) As in A except that the cells also expressed Vph1-mCherry to mark the vacuoles were then treated with either 200 ng/ml or 2.5 ng/ml rapamycin for 3 h. (D) Mutant *pep4Δ prb1Δ-1* (BJ5459) cells harboring cyclin C-YFP and Vph1-mCherry were treated with 200 ng/ml rapamycin for 4 h. Representative fluorescence microscopy images are shown.

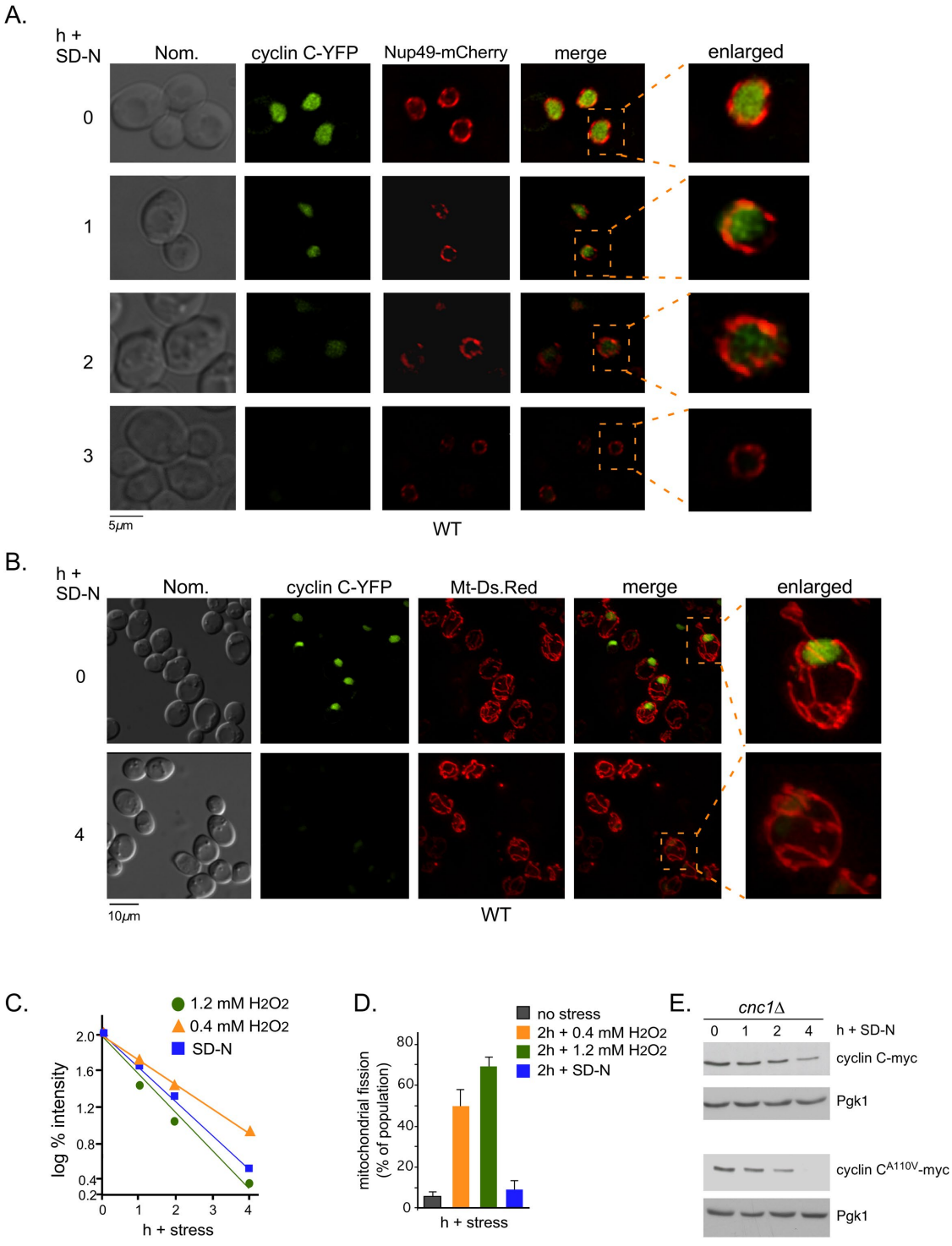

FIGURE 4: Cyclin C does not induce mitochondrial fragmentation following rapamycin stress. (A) Wild-type cells (RSY10) harboring expression plasmids for cyclin C-YFP and Nup49-mCherry were washed and resuspended in SD-N. Representative fluorescence microscopy images of the results are shown. (B) As in A except that the cells also express Mt-Ds-Red to mark the mitochondria. For all panels, Nom. indicates Nomarski imaging. (C) Degradation kinetics of cyclin C after exposure to 1.2 and 0.4 mM H_2O_2 or SD-N as indicated. The data were obtained from previously published experiments (Jin *et al.*, 2015) and Figure 1C. (D) Mitochondrial morphology of cells 2 h after the stress. The data for the H_2O_2 experiments were obtained from (Jin *et al.*, 2015). (E) *cnc1*Δ cells (RSY1696) harboring a wild (pKC337) or cyclin C^{A110V}-myc expression plasmid (pKC354) were grown to mid-log phase and then washed and resuspended in nitrogen starvation medium (SD-N) for the indicated times. Cyclin C-myc levels were monitored by Western blot analysis. Pgk1 levels were used as a loading control.

inhibition triggered by either rapamycin treatment or nitrogen starvation. However, an important difference between the two stressors is that cyclin C destruction occurs prior to an observable cytoplasmic presence or activation of the mitochondrial fission machinery in response to starvation (see *Discussion*). Although the degradation kinetics of cyclin C during H_2O_2 stress (Jin *et al.*, 2014a, 2015) and nitrogen starvation are similar (compared in Figure 4C), a significant increase in mitochondrial fragmentation is only observed following H_2O_2 stress (Jin *et al.*, 2015) (compared with Figure 4D). Moreover, previous studies demonstrated that mitochondrial fragmentation was not observed with a cis mutant (*CNC1*^{A110V}) that does not permit nuclear translocation of cyclin C after H_2O_2 stress (Cooper *et al.*, 2014; Jin *et al.*, 2014a). However, this mutant did not stabilize cyclin C following exposure to nitrogen starvation, indicating that a different signaling system likely triggers cyclin C destruction (Figure 4E). Taken together, these results support the model that nitrogen starvation stimulates cyclin C degradation prior to its detectable presence in the cytoplasm. Consistent with this model, the mitochondria do not exhibit significant stress-induced fragmentation.

Cyclin C-Cdk8 negatively regulates *ATG8* expression within the Ume6-Rpd3 HDAC pathway

Our previous studies identified cyclin C as a repressor of both meiotic and stress response genes (SRG; Cooper *et al.*, 1997, 2012). In yeast, *ATG8* is induced shortly following autophagy stimulation (Kirisako *et al.*, 1999) and encodes a protein that is incorporated into the phagophore membrane to regulate both autophagosome size as well as the binding of selective cargo receptor proteins (Ichimura *et al.*, 2000; Xie *et al.*, 2008). To determine if cyclin C-Cdk8 represses *ATG8* transcription, RT-qPCR analysis was performed on total RNA samples prepared from unstressed yeast *cnc1*Δ and *cdk8*Δ strains. These studies revealed that *ATG8* mRNA levels were increased ~twofold compared with the wild-type control (Figure 5A). Induced levels following 1 h rapamycin treatment were similar in wild-type and mutants cells, indicating that loss of cyclin C-Cdk8 activity was not additive to the normal induction pathway (Figure 5A). GFP-Atg8 protein levels also mirrored these results (Figure 5B, example blot in Supplemental Figure S4A). Furthermore, GFP-Atg8 levels were similarly upregulated in the unstressed *cdk8* kinase dead strain (*cdk8*^{S290A}) (Surosky *et al.*, 1994) (Figure 5C, compare 0 h timepoints). Taken together, these results indicate that cyclin C-Cdk8 kinase activity represses *ATG8* transcription and are consistent with the model that cyclin C destruction is a mechanism to relieve this repression.

To test whether cyclin C-Cdk8 is part of the previously established Ume6-Rpd3 HDAC repression pathway, a series of epistasis experiments was performed. As previously reported (Backues *et al.*, 2012; Bartholomew *et al.*, 2012), RT-qPCR analysis revealed that *ATG8* mRNA levels were elevated ~ fourfold in the *ume6*Δ mutant compared with wild type (compare Figure 4D to Figure 4A).

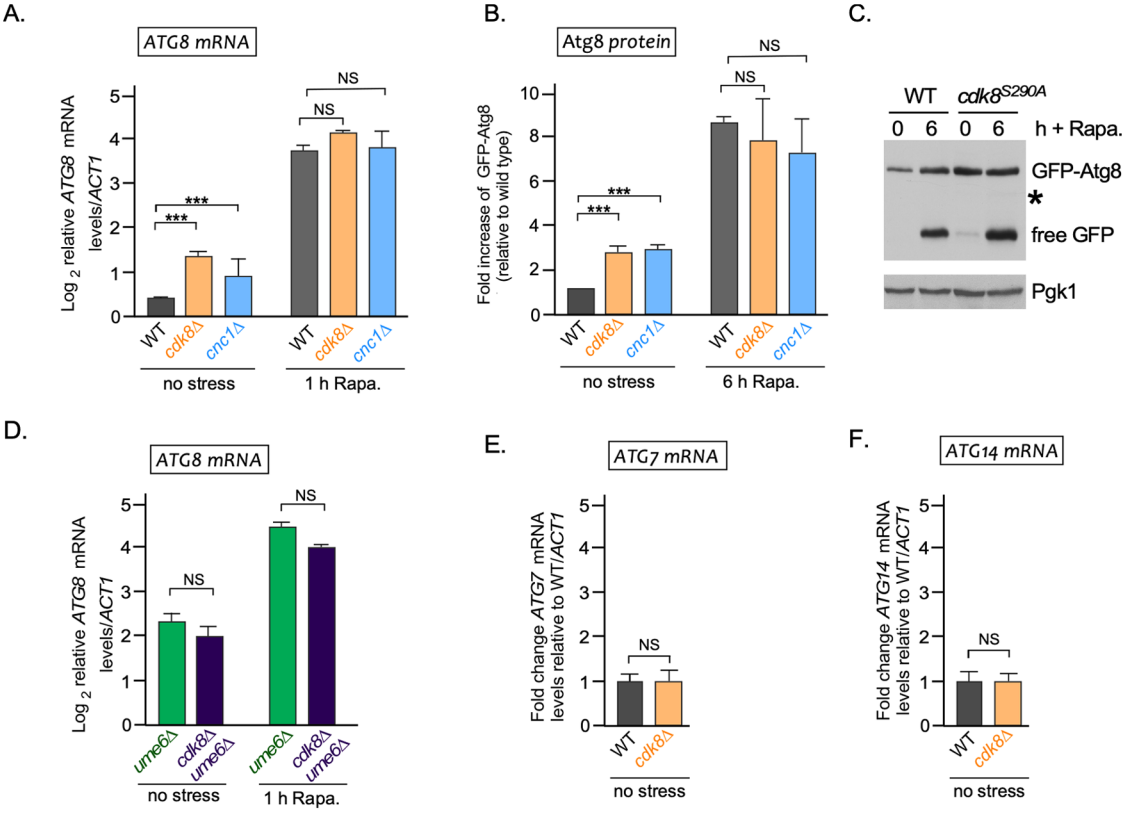

FIGURE 5: Cyclin C-Cdk8 negatively regulates *ATG8* mRNA expression. (A) RT-qPCR assays probing for *ATG8* mRNA expression in the mutant shown before and after 1 h 200 ng/ml rapamycin treatment. Transcript levels are given relative to the internal *ACT1* mRNA control. (B) Fold increase in GFP-Atg8 levels in strains shown before and after 6 h 200 ng/ml rapamycin treatment. (C) GFP-Atg8 cleavage assays before and after 200 ng/ml rapamycin in wild-type (YC7) and *cdk8* kinase dead (YC17) strains. The asterisk indicates a previously reported background band (Huang *et al.*, 2014). (D) As in A for the *ume6*Δ (RSY431) and *ume6 cdk8*Δ (RSY2128) strains as indicated. (E, F) RT-qPCR assays probing for *ATG7* and *ATG14* mRNA expression respectively in wild-type (RSY10) and *cdk8*Δ (RSY1726) unstressed cells. Transcript levels are given relative to the internal *ACT1* mRNA control. For all RT-qPCR assays, the error bars indicate the SD from the mean of two technical replicates from three independent cultures. ***$p < 0.001$ and NS represents no significance.

However, no increase in *ATG8* mRNA levels was observed in the *ume6Δ cdk8Δ* double mutant compared with *ume6Δ* alone. In addition, rapamycin treatment induced a similar increase in *ATG8* mRNA levels in *ume6Δ* and *ume6Δ cdk8Δ* double mutants (Figure 5D). Taken together, these data argue that cyclin C-Cdk8 acts within the Ume6-Rpd3 HDAC pathway to repress *ATG8* transcription. Consistent with this, the mRNA levels of two genes *ATG7* or *ATG14*, which are used to follow autophagy induction and nucleation, respectively (Bernard *et al.*, 2015), but not repressed by Ume6 (Jin *et al.*, 2014b), were also not changed in unstressed *cdk8Δ* cells compared with wild type (Figure 5, E and F). Although this study is not exhaustive, it suggests that Ume6-Rpd3 HDAC and the CKM work together by an unknown mechanism to repress *ATG8* transcription.

Cyclin C-Cdk8 repression restricts cell growth in response to partial TORC1 inhibition

Our epistasis experiments place cyclin C-Cdk8 and Ume6 in the same pathway with regard to *ATG8* repression in replete media. Next, we addressed whether deleting *CDK8* increased autophagic activity as observed in *ume6Δ* mutants (Bartholomew *et al.*, 2012). One method, termed autophagic flux, is based on the finding that GFP is protected from rapid degradation in the vacuole compared with its fusion partner. Therefore, comparing the amount of free GFP cleaved from the non-vacuolar GFP-Atg8 can be used as a measure of autophagic activity (Suzuki *et al.*, 2001; Loos *et al.*, 2014; Delorme-Axford *et al.*, 2015). Quantifying the results described in Figure 5B and Supplemental Figure S4A revealed no significant difference in autophagic flux among wild-type, *cdk8Δ*, and *cnc1Δ* strains (Figure 6A). Another established method of assessing earlier autophagic activity is to determine the amount of substrate being processed through the system as a function of autophagosome formation (Torggler *et al.*, 2017). Using GFP-Atg8 foci as a measure of autophagosome production, we found a significant increase in foci in unstressed *cdk8Δ* and *cnc1Δ* yeast strains compared with wild type (Figure 6B). Taken together, these results suggest that although GFP-Atg8 foci formation increases in *cdk8Δ* and *cnc1Δ*, deletion of the CKM is not sufficient to activate autophagic pathways in the absence of stress.

To further explore the physiological role of cyclin C destruction in the response to nitrogen starvation, we asked whether loss of this repressor enhanced cell survival under nitrogen-limiting conditions. One model consistent with the results from Figure 6, A and B is that the increased number of GFP-Atg8 foci seen in *cnc1Δ* or *cdk8Δ* cells primes them to better survive once autophagy pathways are initiated. Most protocols examining autophagic induction use either total nitrogen starvation or high rapamycin concentrations (e.g., 200 ng/ml) which drives cells into quiescence (Gray *et al.*, 2004;

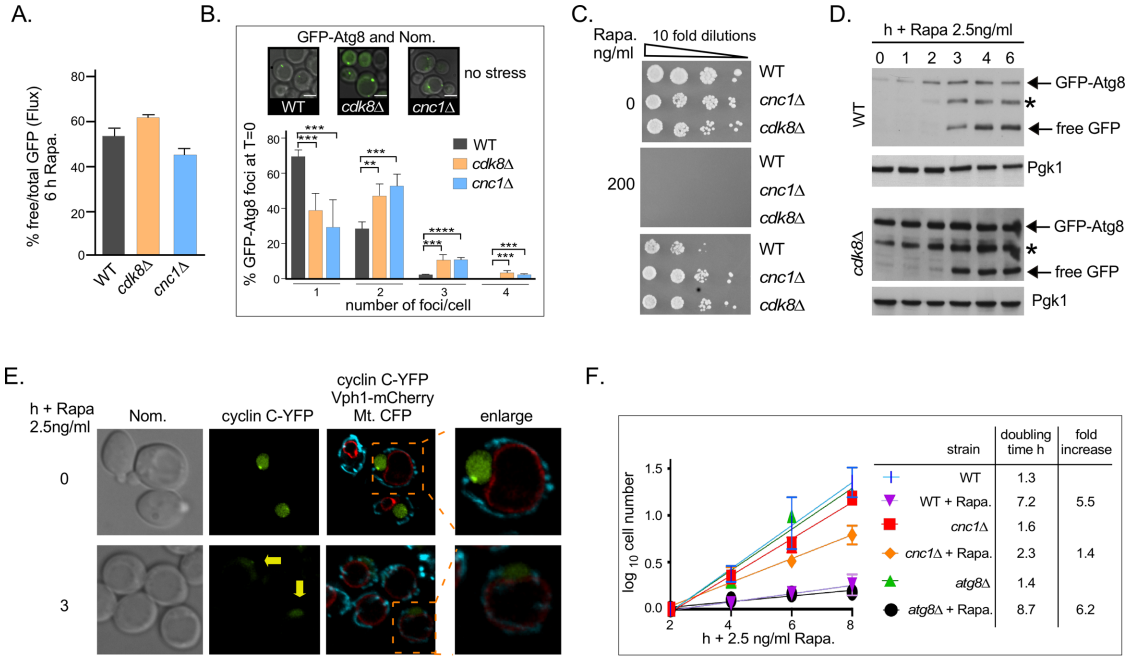

FIGURE 6: Deletion of either *CDK8* or *CNC1* promotes cell survival following low-dose rapamycin treatment. (A) Quantification of GFP-Atg8 flux depicted in Supplemental Supplemental Figure S4A for wild-type (RSY10), *cdk8Δ* (RSY1726) and *cnc1Δ* (RSY1696) cultures. $N = 3$. (B) Representative Nomarski and fluorescence microscopy images of GFP-Atg8 foci are shown for unstressed wild-type, *cnc1Δ*, and *cdk8* cells as in A. Quantification of GFP-Atg8 foci depicted as a percentage of population displaying 0, 1, 2, or 3 foci (percentage of mean ± SD) grown under unstressed conditions. $N = 3$, for all assays: $^{**}p < 0.01$, $^{***}p < 0.001$. $^{****}p < 0.0001$. (C) Wild-type, *cdk8Δ*, and *cnc1Δ* cells were grown to mid log in SD-complete medium and 10-fold dilutions plated on SD-complete medium containing 0, 200, or 2.5 ng/ml rapamycin. (D) Identical exposures of GFP-Atg8 cleavage assays in wild-type and *cdk8Δ* cells after treatment with 2.5 ng/ml rapamycin for the timepoints indicated. The asterisk indicates a previously reported background band (Huang *et al.*, 2014). (E) Wild-type cells (RSY10) harboring expression plasmids for cyclin C-YFP, Vph1-mCherry, and MT. CFP were washed and resuspended in 2.5 ng/ml rapamycin for 3 h. Representative fluorescence microscopy images of the results are shown. Arrows point to detectable cyclin C-YFP after 3 h rapamycin stress. (F) Doubling times of wild type (RSY10), *cnc1Δ* (RSY1696) and *atg8Δ* (RSY2144) cells in YPDA with and without 2.5 ng/ml rapamycin. $N = 3$. (E) For all blots, Pgk1 was used as a loading control.

Narasimhan *et al.*, 2004; Reinke *et al.*, 2006; Klosinska *et al.*, 2011; Waite *et al.*, 2016). As anticipated from these studies, wild-type, *cnc1*Δ, and *cdk8*Δ cells were unable to grow on plates containing 200 ng/ml rapamycin (Figure 6C, middle panel). We thus sought to find the lowest rapamycin concentration that still evoked an autophagic response. We found that 2.5 ng/ml rapamycin induced autophagy using the GFP-Atg8 cleavage assay with kinetics similar to either higher drug concentrations or nitrogen starvation (Figure 6D). Fluorescence microscopy and Western blot analysis showed that cyclin C is also degraded in wild-type cells under these conditions though not to the extent seen at cell-arresting concentrations (200 ng/ml—compare Figure 6E to Figure 3C and see Supplemental Figure S1C). Survival assays on medium containing 2.5 ng/ml rapamycin revealed that the plating efficiency increased in *cnc1*Δ and *cdk8*Δ mutants compared with wild-type controls (Figure 6C, bottom panel). Moreover, a growth rate advantage was also observed in the liquid *cnc1*Δ cultures grown in 2.5 ng/ml rapamycin (doubling time of 2.3 h) compared with wild type grown in 2.5 ng/ml rapamycin (doubling time of 7.2 h, Figure 6F). These findings were most likely due to elevated autophagic activity as *atg8*Δ mutants displayed a significant growth reduction (Figure 6F). These experiments indicate that 2.5 ng/ml rapamycin is sufficient to reduce TORC1 activity to a level that induces autophagy but still permits cell growth, suggesting that this amount of drug triggers a nutrient-limiting, but not eliminated, signal. These experiments also indicate that precocious derepression of the autophagic pathway through *CNC1* or *CDK8* deletion provides cells with a growth advantage under these partial starvation conditions. However, aberrant up-regulation of *ATG8* does not accelerate the timing of autophagic induction as seen by the similar appearance of cleaved GFP-Atg8 in both wild type and the *cdk8*Δ mutant (Figure 6D). Rather, consistent with the GFP-Atg8 foci formation assay (Figure 6A) once autophagy is initiated, the amount of cleaved product increases in the mutant arguing that more substrate is moving through the pathway.

Autophagy induction protects cells from cyclin C-induced mitochondrial fission and cell death following H_2O_2 stress

In controlling the cellular response to oxidative stress, yeast cyclin C has two roles (see Figure 1A). First, along with Cdk8, it represses SRGs in the absence of cell damage. Second, in response to stress, cyclin C performs its Cdk8-independent job by promoting stress-induced mitochondrial fission and RCD. These studies also show that on reaching the cytoplasm, cyclin C mediates mitochondrial fission, even in the absence of stress. This is illustrated by our studies in mammalian cells where *Escherichia coli*-purified yeast GST-cyclin C, but not GST alone, induces mitochondrial fission when added to digitonin-treated mouse embryonic fibroblasts (Wang *et al.*, 2015). In response to nitrogen starvation, cyclin C is still destroyed by the UPS, thereby relieving the repression of *ATG8*. However, our data indicate that cyclin C destruction prevents cytoplasmic accumulation, thus preventing mitochondrial fission following nitrogen starvation. Therefore, one model consistent with these results is that cyclin C proteolysis protects mitochondrial integrity and increases cell survival. Congruous with this hypothesis, amino acid or nitrogen starvation in mammalian cells induces a hyperfused mitochondrial network that promotes cell survival (Rambold *et al.*, 2011b; Gomes and Scorrano, 2013; Morita *et al.*, 2017). To test this model in yeast, wild-type cells were treated with 50 ng/ml rapamycin that induces quiescence similar to the 200 ng/ml concentration described above and destroys cyclin C with similar kinetics (Supplemental Figure S1, A and B). Cyclin C is also degraded using this concentration of rapamycin (Supplemental Figure S1, A and B). Following 0, 2, 3, or 4 h, the cells were subsequently treated with 0.8 mM H_2O_2 for an additional hour. Thereafter, the percentage of cells exhibiting mitochondrial fission and two or more cyclin C-YFP cytoplasmic foci was quantified. The results show that as previously reported (Cooper *et al.*, 2014; Jin *et al.*, 2014a), the addition of H_2O_2 induces cyclin C nuclear translocation and mitochondrial fragmentation (Figure 7A). As anticipated from results presented in Figures 3 and 4, the mitochondria remained reticular even after 4 h of rapamycin stress and cyclin C-YFP was below the limits of detection (Figure 7B). However, increasing the rapamycin exposure time before adding the H_2O_2 reduced both H_2O_2-induced mitochondrial fission and cyclin C-YFP cytoplasmic foci (Figure 7A, quantified in C and D). The addition of H_2O_2 after rapamycin treatment did not affect the appearance of free GFP from GFP-Atg8 in either wild-type or *cdk8*Δ cells (Figure 7E, right panel). Furthermore, similar to a previous report (Perez-Perez *et al.*, 2014), we observed that H_2O_2 stress induces GFP-Atg8 cleavage (Figure 7E, middle panel). This is dependent on autophagy as no cleavage occurs in *atg1*Δ or *atg1*Δ *cnc1*Δ cells (Supplemental Figure S4B). Autophagy, however, is not required for the cytoplasmic translocation of cyclin C following H_2O_2 stress and the mitochondria are able to execute fission in *atg1*Δ cells (Supplemental Figure S4C). Taken together, these results suggest that once autophagy is established, cells are prevented from executing mitochondrial fragmentation. These results are consistent with the model that cyclin C destruction prior to cytoplasmic translocation prevents mitochondrial fragmentation.

To further test the model that rapamycin induced autophagy observed in Figure 7E protects cells from H_2O_2-induced cell death we executed two additional assays. Thereafter either 2 mM H_2O_2 or water was added to the rapamycin treated cells for an additional 2 h. Cell viability was then monitored by plating serial dilutions of the cells on rich medium (YPDA). The results clearly show that pretreatment of the cells with 50 ng/ml rapamycin protects them from 2 mM H_2O_2-mediated cell death. The experiment was repeated by measuring live cells by fluorescein diacetate (FDA) staining and fluorescence activated cell (FACs) analysis. Even after longer exposure times to H_2O_2 (20 h) 4 h pretreatment in rapamycin was protective of cell death with 80% of the H_2O_2-treated cells dying compared with 10% in the pretreated group. These results clearly show that rapamycin protects cells from H_2O_2-mediated cell death.

Mitochondrial cyclin C localization triggers cell death following autophagy induction

The experiments described above are consistent with a model that preventing cyclin C–mitochondrial interaction increases cell survival in response to starvation conditions. Previously, we have shown that deleting *MED13*, the gene encoding the nuclear anchor for cyclin C, allows constitutive cyclin C cytoplasmic localization and mitochondrial fragmentation (Khakhina *et al.*, 2014). Importantly, these results, as well as those obtained in mammalian cells (Jezek *et al.*, 2019a), showed that simply placing cyclin C at the mitochondria does not induce RCD in the absence of stress but does make the cells hypersensitive to cell damage. In other words, yeast and mammalian cells undergo RCD more efficiently when cyclin C is located at the mitochondria before the stress. To test the possibility that preventing cyclin C from reaching the mitochondria may help increase survival upon starvation conditions, we constructed a chimeric gene fusing the outer mitochondrial membrane (OMM)-associating domain of Fis1 to the C terminus of cyclin C-YFP (called cyclin C-YFP-Fis). Fis1 is the receptor for the GTPase Dnm1-Mdv1 complex required for mitochondrial fission (Tieu and Nunnari, 2000; Karren *et al.*, 2005; Bhar *et al.*, 2006). As expected, fluorescence

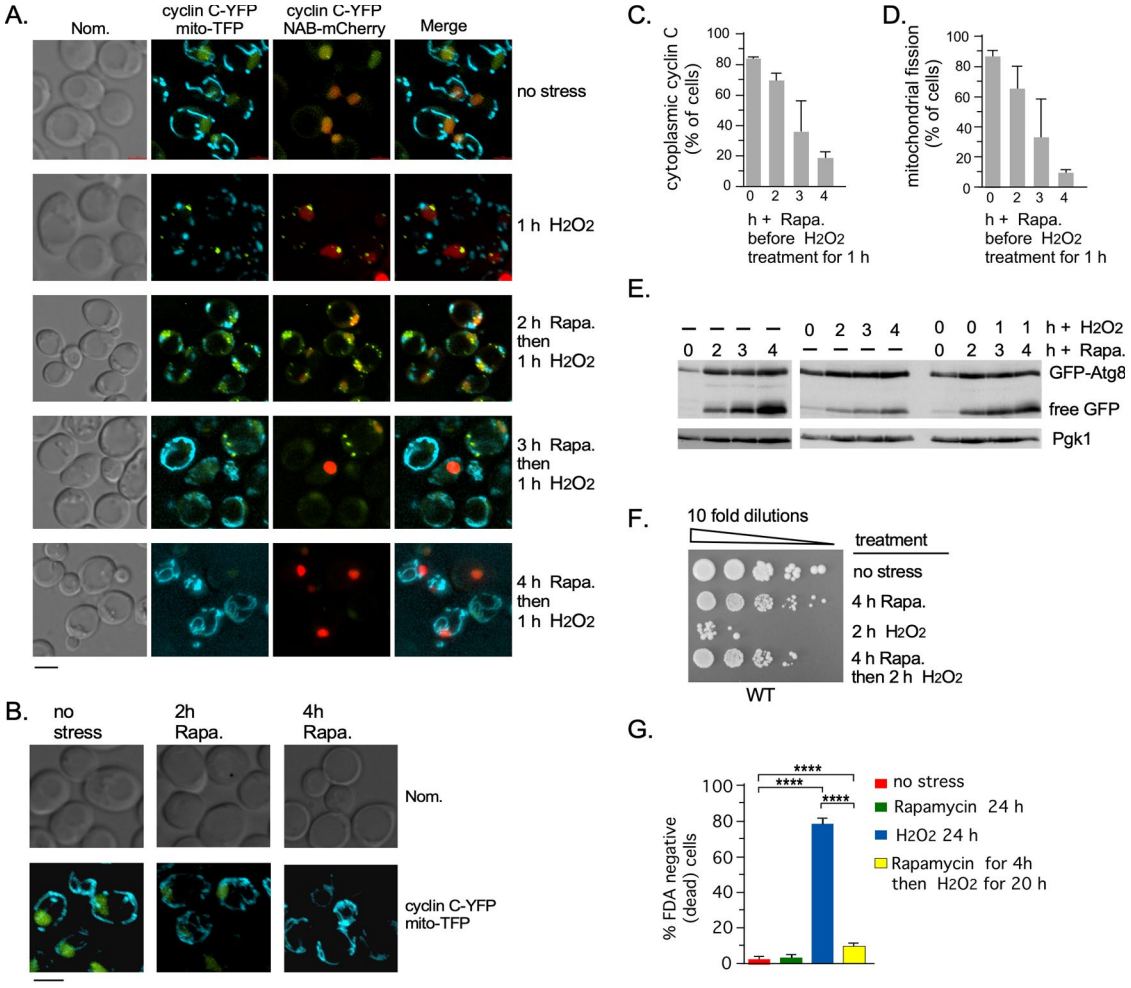

FIGURE 7: Rapamycin treatment protects mitochondria from H_2O_2-mediated fragmentation. (A) Wild-type cells harboring the plasmids shown were grown to mid-log and treated with 50 ng/ml rapamycin and thereafter 0.8 mM H_2O_2 for the times indicated. Representative fluorescence microscopy images of the results are shown. Bar = 5 µm. (B) Representative images of cells from A treated with 50 ng/ml rapamycin. Bar = 5 µm. (C, D) The percentage of cells from A that had cytoplasmic cyclin C and fragmented mitochondria respectively. $N = 3$. (E) GFP-Atg8 cleavage assays following treatment with 50 ng/ml rapamycin (left panel) or 0.8 mM H_2O_2 (middle panel) for the timepoints indicated. In the right-hand panel, H_2O_2 was added for 1 h after rapamycin addition. (F) Mid-log wild-type cells were subjected to the conditions shown (50 ng/ml rapamycin and 2 mM H_2O_2) and thereafter cell viability determined by growth (10-fold dilutions) on rich medium (YPDA). (G) Mid-log wild-type cells were treated as described in F except that except that the % of live cells was monitored by FDA staining and FACs analysis after 24 h. The % of dead cells (FDA negative) was graphed for each condition. $N = 3$. ****$p < 0.0001$.

microscopy revealed that cyclin C-YFP-Fis localized to the OMM and this fusion protein is sufficient to induce mitochondrial fragmentation in the absence of a stress signal (Figure 8A, quantified in B and C).

Next, we addressed whether redirecting cyclin C to the mitochondria affects cell survival in response to rapamycin stress. The survival assay described above (Figure 6C) was repeated using *cnc1*Δ cells expressing either cyclin C-YFP or cyclin C-YFP-Fis. Compared to the cyclin C-YFP control, cells harboring the cyclin C-YFP-Fis construct exhibited approximately a 10-fold decrease in viability on 2.5 ng/ml rapamycin plates (Figure 8C). This result supports a model that cyclin C localization to the mitochondria reduces survival during starvation. To address this question another way, we took advantage of the *med13*Δ mutation that allows constitutive cyclin C nuclear release in the absence of stress (Khakhina *et al.*, 2014). In terms of mitochondrial morphology, unstressed *med13*Δ have fragmented mitochondria, whereas double *cnc1*Δ *med13*Δ mutants restore this organelle to a reticular phenotype. Here we tested if wild type, *cnc1*Δ, *med13*Δ, and *cnc1*Δ *med13*Δ exhibited viability differences following nitrogen starvation using a standard autophagy survival assay (Noda, 2008). Cells were switched to nitrogen starvation medium then viability determined by using phloxine B staining that identifies dead cells. As previous studies have shown, cell viability in *atg* mutants decreases ~50% after 72 h following nitrogen starvation compared with 10% for wild-type cells (Shpilka *et al.*, 2015). Similarly, 10% of the wild-type population was phloxine B positive after 3 d in nitrogen starvation medium (Figure 8E). A similar result was seen for *cnc1*Δ mutants. However, we found that the percentage of phloxine B-positive cells was significantly elevated in *med13*Δ mutants after 3 d of nitrogen starvation (Figure 8E). Importantly, the *med13*Δ-dependent cell death elevation required cyclin C as deleting *CNC1* mostly suppressed this

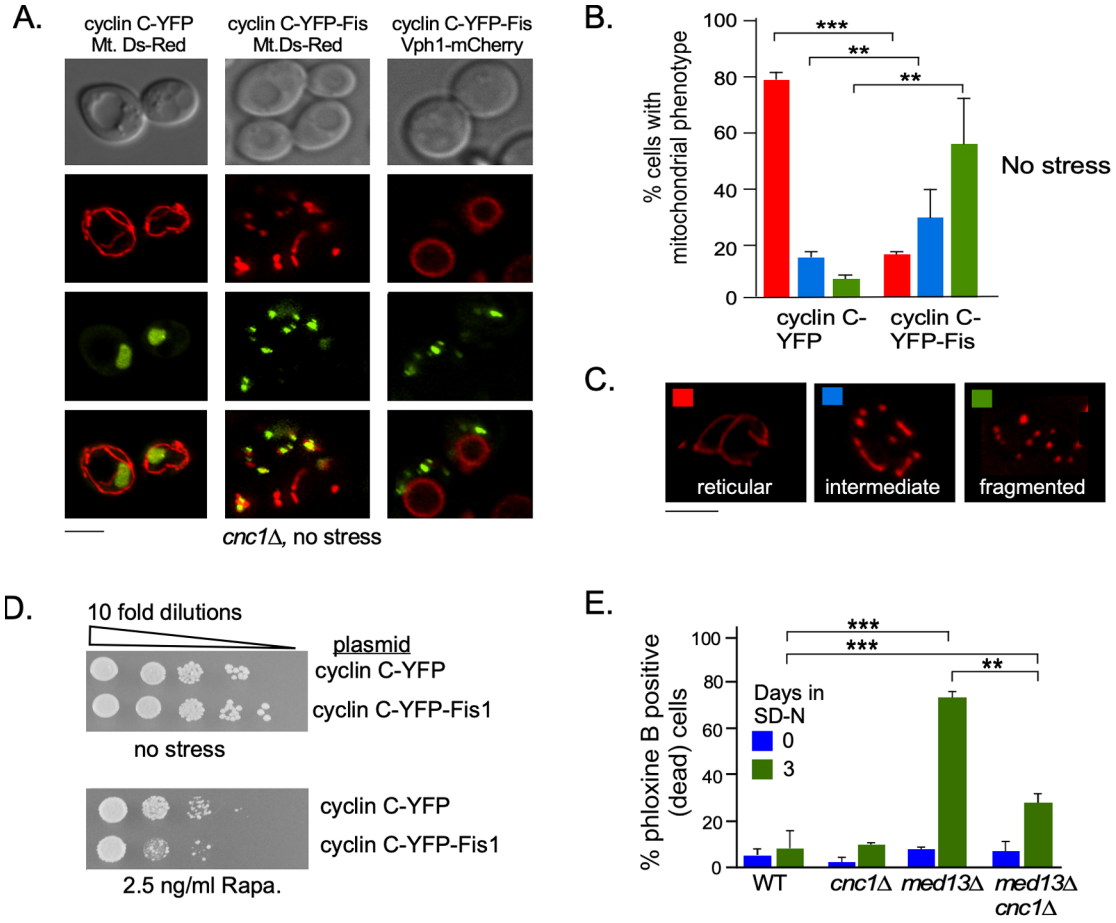

FIGURE 8: Redirecting cyclin C to the mitochondria promotes cell death in response to survival signals. (A) Fluorescence microscopy of mid-log phase *cnc1*Δ cells harboring expression plasmids for either cyclin C-YFP or the cyclin C-YFP-Fis chimeric protein plus either the mitochondria or the vacuole markers (Mt. Ds-Red and Vph1-mCherry, respectfully). Bar = 5 μm. The top panels are Nomarski images. (B) Quantification of mitochondrial morphology in *cnc1*Δ cells harboring either cyclin C-YFP or cyclin C-YFP-Fis expression plasmids. At least 200 cells were counted from three individual isolates. The percentage of cells (mean ± SD) within the population displaying the different mitochondrial morphologies is given. (C) Representative fluorescence microscopy images of the mitochondrial morphologies scored in B. Bar = 5 μm. (D) Survival assays as described in Figure 6C in *cnc1*Δ cells harboring either cyclin C-YFP or cyclin C-YFP-Fis expression plasmids. (E) Mid-log cells with the genotypes shown were washed then switched to SD-N medium. The percent of inviable cells within the population was determined using phloxine B staining and FACs analysis after 3 days. $N = 3$. For all experiments $^{**}p < 0.01$, $^{***}p < 0.001$.

phenotype. Taken together, these results support a model that rapidly destroying cyclin C by the UPS restricts it from translocating to the cytoplasm following nitrogen starvation, thereby preventing mitochondrial fragmentation and RCD (see *Discussion*). Therefore, manipulating the location of a single protein allows the cell to quickly adapt to changing environmental cues such as oxidative stress or nitrogen starvation to deliver the correct molecular response.

DISCUSSION

Correctly adapting to environmental signals requires the cell to translate signals into a molecular response. Previous studies have shown that this response triggers a change in mitochondria morphology, with fragmented mitochondria preceding RCD, while hyper-elongated mitochondria are found in cells destined to survive. Here we describe how the fate of a nuclear protein, cyclin C, helps direct which path the cell follows dependent on the input stimulus. A model that best fits the data is shown in Figure 9. In unstressed cells (left-hand panel), cyclin C is nuclear and by activating its cognate kinase Cdk8 (not shown) represses a subset of SRGs. In response to oxidative stress (middle panel), cyclin C-dependent repression is relieved by translocating out of the nucleus where it is destroyed by the UPS, mediated by the Not4 E3 ligase. A similar strategy is taken to relieve cyclin C-Cdk8 repression of *ATG8* following nitrogen starvation in that cyclin C is also destroyed by the UPS, utilizing the 26S proteasome accompanied by a different E3 ligase. However, we uncovered an important difference between these two pathways. Significantly, although cyclin C degradation kinetics are similar between H_2O_2 and nitrogen depletion stress (see Figure 4C), no detectable cytoplasmic cyclin C is observed following starvation. As a result, the mitochondria are protected from cyclin C mediated fragmentation and remain elongated eliciting a survival response. This model is supported by our finding that simply redirecting cyclin C to the mitochondria shifts the starvation response from survival to death (Figure 8). Taken together, these results imply that the subcellular address of cyclin C is directed by environmental cues and plays

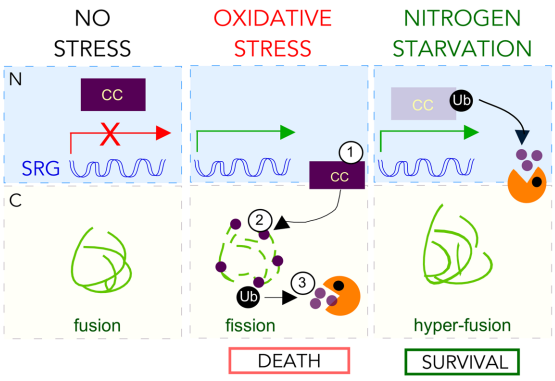

FIGURE 9: Model for regulator network controlling the final subcellular address for cyclin C and subsequent cell fate decisions. In unstressed cells growing in replete media (left-hand panel), cyclin C-Cdk8 repress the expression of a subset of stress-responsive genes; 80–90% of the mitochondria show a reticular fused phenotype. After treatment with H_2O_2 (middle panel), cyclin repression on cyclin C–Cdk8-controlled genes is relieved by cyclin C translocation to the cytoplasm (1). There it interacts with the fission machinery (and Bax in mammalian cells) to induce stress-induced mitochondrial fission and promote cell death (2). Thereafter, cyclin C is destroyed by the UPS dependent on the Not4 E3 ligase. Following nitrogen depletion (right panel), the cyclin C-Cdk8 repression of the autophagy gene *ATG8* is relieved by destroying cyclin C before it can affect mitochondrial morphology (possibly in the nucleus or at the NPC) by the UPS system. The 26S proteasome and an unknown E3 ligase(s) are required. As a result, the mitochondria remain reticular or may even become hyper-elongated to promote ATP production under starvation conditions. *N* = nucleus, C = cytoplasm.

a role in directing cell fates. Combined with our previous studies (Cooper *et al.*, 1997, 2014), these results demonstrate that cyclin C's role as a repressor of SRGs is identical following both survival and cell death cues, whereas it only mediates mitochondrial fragmentation in response to cell death cues.

Although the exact location of cyclin C destruction following nitrogen starvation was not determined, these studies imply that it is different from oxidative stress. Exactly where active proteasomes are located is still controversial and was recently reviewed (Enenkel, 2014). Solid genetic experiments with nuclear and cytoplasmic substrates suggest that active proteasomes are located on the outside of the NPC (Chen and Madura, 2014). Similar genetic approaches by others with different substrates suggest that proteasomes destroy substrates in the nucleus (Boban *et al.*, 2014). Likewise, Ump1-GFP, and other proteasomal subunits, have been reported to primarily localize to the nucleus in dividing cells (Lehmann *et al.*, 2002; Fehlker *et al.*, 2003). Last, it has been suggested that active proteasomes are located in clusters surrounding the NPC (Chen and Madura, 2014; Albert *et al.*, 2017), which may help resolve the conflicting data obtained by different groups. Further studies with cyclin C may not only be useful in understanding how the CKM controls the response to various stresses but also could be used as a test substrate to investigate what cellular compartment maintain active proteasomes. It was interesting that the cyclin C mutation (A110V) that stabilizes cyclin C in the nucleus in response to oxidative stress (Jin *et al.*, 2014a) did not have the same effect following nitrogen starvation. This same mutation also partially stabilizes cyclin C following heat shock where cytoplasmic foci are seen and during meiosis (Cooper and Strich, 1999; Cooper *et al.*, 1997, 2012). This suggests that different upstream signaling systems are at play to redirect CKM components dependent on the stress.

Cyclin C destruction following nitrogen depletion promotes cell survival by up-regulation of *ATG8* transcription

Why does cyclin C destruction promote cell survival following nitrogen starvation? We propose that there are two main explanations for this observation. First, destroying cyclin C inactivates its cognate kinase Cdk8, promoting induction of the essential autophagy gene *ATG8*. The studies presented here, combined with those of others, show that *ATG8* derepression upon nitrogen starvation requires multiple steps. First, Ume6 function is negated on phosphorylation by the great wall kinase Rim15 (Backues *et al.*, 2012). Epistasis experiments place cyclin C-Cdk8 into this pathway in an unknown role. Consistent with this model, both cyclin C-Cdk8 (Figure 5) and Ume6 do not regulate *ATG7* or *ATG14* mRNA expression (Jin *et al.*, 2014b). One possibility is that this kinase phosphorylates a member of the Ume6–HDAC complex that in turn maintains *ATG8* repression. An alternative, but not mutually exclusive possibility, is that cyclin C-Cdk8 represses Rim15 activity. Two targets of this pathway are the transcriptional activators Msn2-Msn4 which up-regulate *ATG8* expression by an unknown mechanism upon starvation (Vlahakis *et al.*, 2017). Although we currently do not understand the precise molecular mechanism, the results presented here show that that precocious *ATG8* induction in the absence of cyclin C-Cdk8 provides a growth advantage. Importantly, this growth advantage was dependent on autophagy induction, as it was not observed in *atg8*Δ cells (Figure 6). This suggests a model in which the increased GFP-Atg8 foci seen in *cnc1*Δ or *cdk8*Δ cells primes them to deal with starvation conditions, but an external starvation signal is required to trigger autophagic activity. Last, although these results show that cyclin C-Cdk8 regulate *ATG8*, it is possible that this kinase could negatively regulate other autophagy genes. Consistent with this, Cdk8 was identified in a recent proteomics screen as a negative regulator of general autophagy (Müller *et al.*, 2015). Different to our experiments, here autophagic activity was measured after 24 h rapamycin stress using the alkaline phosphatase-based assay which utilizes a cytosol-targeted proenzyme of ALP (cytALP) (Mendl *et al.*, 2011).

Cyclin C destruction following nitrogen depletion promotes cell survival by inhibiting extensive mitochondrial fragmentation

Results presented in this paper argue that the second reason for cyclin C destruction following nitrogen starvation is to prevent mitochondrial fission. As cyclin C-mediated mitochondrial fission promotes H_2O_2-induced RCD, the simplest interpretation would be that preventing cyclin C–mitochondrial association promotes the autophagic response over the death program (see Figure 9). This model is strongly supported by our finding that misdirecting cyclin C to the mitochondria changes the starvation signal from survival to death. The relationship between mitochondrial morphology and cell survival has been studied in mammalian cells (Rambold *et al.*, 2011a; Gomes and Scorrano, 2013). In these studies, autophagy induction by starvation or mTORC1 inhibition stimulates mitochondria hyperfusion. As a result, mitochondria possess more cristae which in turn optimizes ATP production (Buck *et al.*, 2016; Gandin *et al.*, 2016; Mishra and Chan, 2016), thereby linking mitochondrial dynamics to the metabolic state of the cell (Morita *et al.*, 2017). This protective effect of mTORC1 inhibition against oxidative stress is also evident in reactive oxygen species-associated pathologies such as aging and neurodegenerative diseases (Rubinsztein *et al.*, 2011), playing a role in

maintaining long-term fitness of cells, predominantly by up-regulating transcriptional responses that support adaptation (Aramburu *et al.*, 2014). However, the role mitochondria play is just starting to emerge (Sun *et al.*, 2016; Srivastava, 2017) with recent studies showing that inhibition of mitochondrial fission attenuates disease progression in models of neurodegenerative and cardiovascular diseases (Cui *et al.*, 2010; Givvimani *et al.*, 2012; Ong *et al.*, 2010). Mitophagy is also attenuated in cells with reduced mitochondrial fission, suggesting that fission is a prerequisite for mitophagy to occur (Arnoult *et al.*, 2005; Lee *et al.*, 2011; Liu *et al.*, 2020). Likewise, it is not completely understood how mitochondrial dynamics affect cell death mechanisms (Liu *et al.*, 2020). However, our results in mammalian cells strongly suggest that cyclin C plays a role, as it binds to Drp1 following stress (Ganesan *et al.*, 2019). Moreover, we also found that cyclin C also associates directly with Bax (Jezek *et al.*, 2019a), affirming its previously characterized role in regulating MOMP and intrinsic cell death mechanisms (Wang *et al.*, 2015). Given the identification of cyclin C as a tumor suppressor (Li *et al.*, 2014; Jezek *et al.*, 2019c) and the contradictory role of autophagy as a mechanism that both promotes and inhibits tumorigenesis (Lorente *et al.*, 2018), this work emphasizes the need for further studies to investigate cyclin C's role in promoting survival in response to nutrient depletion in mammals.

MATERIALS AND METHODS

Yeast strains and plasmids

Experiments performed primarily in the *S. cerevisiae* W303 background (Ronne and Rothstein, 1988) are listed in Supplemental Table S2 and have an RSY prefix. Experiments performed in different strain backgrounds are noted in the figure legend. In accordance with the Mediator nomenclature unification efforts (Bourbon *et al.*, 2004), the cyclin C (*SSN8*/*UME3*/*SRB11*) and Cdk8 (*SSN3*/*UME5*/*SRB10*) will use *CNC1* and *CDK8* gene designations, respectively. Plasmids used in this study are listed in Supplemental Table S3. Plasmids construction details are available on request. All constructs were verified by sequencing. The previously described transmembrane domain of Fis1 (amino acids 121–155; Horie *et al.*, 2003) was used to construct the cyclin C-YFP-Fis1 chimeric protein.

Yeast cell growth

Yeast were grown in either rich, nonselective medium (YPDA: 2% [wt/vol] glucose, 2% (w/v) Bacto peptone, 1% (w/v) yeast extract, 0.001% (w/v) adenine sulfate or synthetic minimal dextrose (SD: 0.17% [wt/vol] yeast nitrogen base without amino acids and ammonium sulfate, 0.5% [wt/vol] ammonium sulfate, 1× supplement mixture of amino acids, 2% [wt/vol) glucose) allowing plasmid selection as previously described (Cooper *et al.*, 1997). For all experiments, the cells were grown to mid-log phase (~6×10^6 cells/ml) in 2% glucose media selecting for plasmids when appropriate before directly adding rapamycin (Biovision, dissolved in 90% Tween, 10% ethanol) or 0.8 mM H_2O_2 (Millipore Sigma HX0635-3) at the concentrations indicated into the SD media. For the nitrogen starvation experiments, mid-log phase cells were washed in H_2O then resuspended in synthetic dextrose medium lacking ammonium sulfate or supplemental amino acids (SD-N). Protein extracts were prepared from 25-ml culture samples per timepoint and washed in H_2O, and the pellet was flash frozen in liquid nitrogen (see below for more details). *E. coli* cells for isolating plasmids were grown in LB medium with selective antibiotics as previously described (Cooper *et al.*, 1997). For the rapamycin survival assays (Figures 6C and 8C), mid-log cells were grown in YPDA medium, serially diluted 10-fold, and then plated onto SD complete plates containing either 200 or 2.5 ng/ml rapamycin. For growth rate studies (Figure 6F), strains were grown in YPDA to 2×10^5 cells/ml and then followed for 6 h after the addition of 2.5 ng/ml rapamycin. For the cycloheximide chase assay (Supplemental Figure S1E), mid-log phase cells were treated with 50 µg/ml cycloheximide dissolved in dimethyl sulfoxide for 4 h.

Yeast cellular assays

RT-qPCR analysis was executed as previously described (Cooper *et al.*, 2012). Oligonucleotides used are available on request. All RT-qPCR studies were conducted with three biological samples in technical duplicates. For all other assays, the experiments were performed in biological replicates and the number of replicates for each experiment is given in the figure legends. *P* values were determined using the Student's *t* test. GFP-Atg8 cleavage assays were executed as described (Nair *et al.*, 2011) using the single-copy GFP-Atg8 expression plasmid (Abeliovich *et al.*, 2003) except that protein extracts were prepared using the NaOH lysis method described below. For the three (Figure 8D), the cells were grown in SD, washed, and then resuspended in SD-N. After 3 d, the cells were stained with phloxine B (Millipore Sigma P2759) at 5 µg/ml essentially as described (Noda, 2008). The percentage of phloxine positive (dead) cells was measured using FACs as previously described (Khakhina *et al.*, 2014). To determine cell viability in Figure 7G, the cells were stained, grown in SD medium to mid-log, split into four, and treated as shown. H_2O_2 was added directly to rapamycin-treated cells at the time indicated. After the treatment, the cells were spun down and resuspended in phosphate-buffered saline and stained with FDA (Millipore Sigma P7378) at 10 µg/ml essentially as described (Kwolek-Mirek and Zadrag-Tecza, 2014). The percentage of FDA-positive (live cells) was analyzed by FACs and plotted as the amount of unstained (dead) cells. For both FDA and phloxine stains, 30,000 cells were counted per timepoint and samples were analyzed in biological triplicate. The plating assay shown in Figure 7F was essentially executed in a similar manner. The cells were grown in SD to mid-log, split, and treated as shown in the figure with H_2O_2 being added to rapamycin-treated cells. After the time shown, 10-fold dilutions of the cells were made and plated on YPDA media.

Western blot analysis

Protein extracts for Western blot studies were prepared using a NaOH lysis procedure exactly as described (Stieg *et al.*, 2018; Willis *et al.*, 2018). To detect epitope tagged proteins 1:5000 dilutions of all primary antibodies were used (anti-myc [UpState New York], anti-HA and anti-GFP [Abcam]) except that 1:2500 dilutions of anti-Pgk1 (Invitrogen) antibodies were used. Western blot signals were detected using 1:5000 dilutions of either goat anti-mouse or goat anti-rabbit secondary antibodies conjugated to alkaline phosphatase (Abcam) and the CDP-Star chemiluminescence kit (Thermo). Signals were quantified (relative to Pgk1 controls) by CCD camera imaging (Kodak). All degradation assays were performed more than once on biological replicates (see figure legends for the exact number). The SD was calculated from the mean (error bars) using GraphPad Prism 7. The half-life of cyclin C degradation was calculated from these graphs.

E3 ligase screen

The putative E3 ligases screened are listed in Supplemental Table S1 and were previously identified by others (Finley *et al.*, 2012;

Zhu *et al.*, 2016). Viable null mutants from the yeast knockout collection (Chu and Davis, 2008) were transformed with cyclin C-myc (pLR101) and were starved of nitrogen for 4 h. Cyclin C was detected by Western blot analysis as described above and images were quantified as described above. The blots were stripped and probed for Pgk1. A representative Western blot image is shown in Supplemental Figure S2E. To create the *rsp5* end-N rule doxycycline inducible degron (Supplemental Figure S2A), pMK632 was integrated into cells to create RSY2301 (Ubi-leucine::3HA-Rsp5). Next, RSY2301, harboring cyclin C-myc, was grown to low mid-log, a sample was removed to control for Rsp5-HA expression, and then treated with 2 µg/ml doxycycline (Sigma D9891) for 5 h. Thereafter, the cells were washed in water and resuspended in SD-N plus doxycycline and samples were taken for NaOH lysis and Western analysis as described above. The same method was used to create the *skp1* and *tfb3* end-N rule degron strains, except that pMK-Arg was integrated into cells to create RSY2366 and RSY2367, respectively.

Fluorescence microscopy

YFP-cyclin C subcellular localization and mitochondrial morphology was monitored as described previously (Cooper *et al.*, 2012, 2014). For all experiments, the cells were grown to mid-log (6×10^6 cells/ml), treated with either H_2O_2, rapamycin, or resuspended in SD-N (after being washed in water) for the timepoints indicated, then analyzed by fluorescence microscopy. Images were obtained using a Nikon 90i microscope with a 100× objective with 1.2× camera magnification (Plan Fluor Oil, NA 1.3) and a CCD camera (Hamamatsu model C4742). Data were collected using NIS software and processed using Image Pro software. All images of individual cells were optically sectioned (0.2-µm slices at 0.3-µm spacing) and deconvolved, and the slices were collapsed to visualize the entire fluorescent signal within the cell. Cyclin C-YFP foci were scored as being cytoplasmic when three or more foci were observed outside of the nucleus (Jin *et al.*, 2014a). Mitochondrial fission assays were performed on live cells as described (Cooper *et al.*, 2014). In brief, mitochondrial fission was scored positive if no reticular mitochondria were observed that transversed half the cell diameter. Fusion was scored when cells exhibited one or more reticular mitochondria the diameter of the cell. Fission and fusion was scored for 200 cells from three independent isolates. GFP-Atg8 foci were scored in unstressed cells for at least 200 cells from three independent isolates as described (Torggler *et al.*, 2017). Statistical analysis was performed using the Student's *t* test.

ACKNOWLEDGMENTS

We thank A. Alberti, R. Deshaies, D. Finely, P. Herman, M. Hochstrasser, E. Jones, and K. Madura for strains and plasmids. We especially thank members of the Cooper laboratory and R. Strich for critical reading of this manuscript. This work was supported by a grant from the National Institutes of Health awarded to K.F.C. (GM113196).

REFERENCES

Abeliovich H, Zhang C, Dunn WA Jr, Shokat KM, Klionsky DJ (2003). Chemical genetic analysis of Apg1 reveals a non-kinase role in the induction of autophagy. Mol Biol Cell 14, 477–490.

Albert S, Schaffer M, Beck F, Mosalaganti S, Asano S, Thomas HF, Plitzko JM, Beck M, Baumeister W, Engel BD (2017). Proteasomes tether to two distinct sites at the nuclear pore complex. Proc Natl Acad Sci USA 114, 13726–13731.

Allen BL, Taatjes DJ (2015). The Mediator complex: a central integrator of transcription. Nat Rev Mol Cell Biol 16, 155–166.

Aramburu J, Ortells MC, Tejedor S, Buxade M, Lopez-Rodriguez C (2014). Transcriptional regulation of the stress response by mTOR. Sci Signal 7, re2.

Arnoult D, Rismanchi N, Grodet A, Roberts RG, Seeburg DP, Estaquier J, Sheng M, Blackstone C (2005). Bax/Bak-dependent release of DDP/TIMM8a promotes Drp1-mediated mitochondrial fission and mitoptosis during programmed cell death. Curr Biol 15, 2112–2118.

Bachmair A, Finley D, Varshavsky A (1986). In vivo half-life of a protein is a function of its amino-terminal residue. Science 234, 179–186.

Backues SK, Lynch-Day MA, Klionsky DJ (2012). The Ume6-Sin3-Rpd3 complex regulates ATG8 transcription to control autophagosome size. Autophagy 8, 1835–1836.

Bartholomew CR, Suzuki T, Du Z, Backues SK, Jin M, Lynch-Day MA, Umekawa M, Kamath A, Zhao M, Xie Z, *et al.* (2012). Ume6 transcription factor is part of a signaling cascade that regulates autophagy. Proc Natl Acad Sci USA 109, 11206–11210.

Bernard A, Jin M, Gonzalez-Rodriguez P, Fullgrabe J, Delorme-Axford E, Backues SK, Joseph B, Klionsky DJ (2015). Rph1/KDM4 mediates nutrient-limitation signaling that leads to the transcriptional induction of autophagy. Curr Biol 25, 546–555.

Bhar D, Karren MA, Babst M, Shaw JM (2006). Dimeric Dnm1-G385D interacts with Mdv1 on mitochondria and can be stimulated to assemble into fission complexes containing Mdv1 and Fis1. J Biol Chem 281, 17312–17320.

Bjorklund S, Gustafsson CM (2005). The yeast Mediator complex and its regulation. Trends Biochem Sci 30, 240–244.

Boban M, Pantazopoulou M, Schick A, Ljungdahl PO, Foisner R (2014). A nuclear ubiquitin-proteasome pathway targets the inner nuclear membrane protein Asi2 for degradation. J Cell Sci 127, 3603–3613.

Bourbon HM, Aguilera A, Ansari AZ, Asturias FJ, Berk AJ, Bjorklund S, Blackwell TK, Borggrefe T, Carey M, Carlson M, *et al.* (2004). A unified nomenclature for protein subunits of mediator complexes linking transcriptional regulators to RNA polymerase II. Mol Cell 14, 553–557.

Braun RJ, Westermann B (2011). Mitochondrial dynamics in yeast cell death and aging. Biochem Soc Trans 39, 1520–1526.

Bucci M, Wente SR (1997). In vivo dynamics of nuclear pore complexes in yeast. J Cell Biol 136, 1185–1199.

Buck MD, O'Sullivan D, Klein Geltink RI, Curtis JD, Chang CH, Sanin DE, Qiu J, Kretz O, Braas D, van der Windt GJ, *et al.* (2016). Mitochondrial dynamics controls T cell fate through metabolic programming. Cell 166, 63–76.

Buttner S, Eisenberg T, Carmona-Gutierrez D, Ruli D, Knauer H, Ruckenstuhl C, Sigrist C, Wissing S, Kollroser M, Frohlich KU, *et al.* (2007). Endonuclease G regulates budding yeast life and death. Mol Cell 25, 233–246.

Cardenas ME, Cutler NS, Lorenz MC, Di Como CJ, Heitman J (1999). The TOR signaling cascade regulates gene expression in response to nutrients. Genes Dev 13, 3271–3279.

Cebollero E, Reggiori F (2009). Regulation of autophagy in yeast Saccharomyces cerevisiae. Biochim Biophys Acta 1793, 1413–1421.

Chen L, Madura K (2014). Degradation of specific nuclear proteins occurs in the cytoplasm in Saccharomyces cerevisiae. Genetics 197, 193–197.

Chu AM, Davis RW (2008). High-throughput creation of a whole-genome collection of yeast knockout strains. Methods Mol Biol 416, 205–220.

Conrad M, Schothorst J, Kankipati HN, Van Zeebroeck G, Rubio-Texeira M, Thevelein JM (2014). Nutrient sensing and signaling in the yeast Saccharomyces cerevisiae. FEMS Microbiol Rev 38, 254–299.

Cooper KF, Khakhina S, Kim SK, Strich R (2014). Stress-induced nuclear-to-cytoplasmic translocation of cyclin C promotes mitochondrial fission in yeast. Dev Cell 28, 161–173.

Cooper KF, Mallory MJ, Smith JB, Strich R (1997). Stress and developmental regulation of the yeast C-type cyclin Ume3p (Srb11p/Ssn8p). EMBO J 16, 4665–4675.

Cooper KF, Mallory MJ, Strich R (1999). Oxidative stress-induced destruction of the yeast C-type cyclin Ume3p requires phosphatidylinositol-specific phospholipase C and the 26S proteasome. Mol Cell Biol 19, 3338–3348.

Cooper KF, Scarnati MS, Krasley E, Mallory MJ, Jin C, Law MJ, Strich R (2012). Oxidative-stress-induced nuclear to cytoplasmic relocalization is required for Not4-dependent cyclin C destruction. J Cell Sci 125, 1015–1026.

Cooper KF, Strich R (1999). Functional analysis of the Ume3p/ Srb11p-RNA polymerase II holoenzyme interaction. Gene Expr 8, 43–57.

Cui M, Tang X, Christian WV, Yoon Y, Tieu K (2010). Perturbations in mitochondrial dynamics induced by human mutant PINK1 can be rescued by the mitochondrial division inhibitor mdivi-1. J Biol Chem 285, 11740–11752.

Czabotar PE, Westphal D, Dewson G, Ma S, Hockings C, Fairlie WD, Lee EF, Yao S, Robin AY, Smith BJ, *et al.* (2013). Bax crystal structures reveal how

BH3 domains activate Bax and nucleate its oligomerization to induce apoptosis. Cell 152, 519–531.
Daulny A, Geng F, Muratani M, Geisinger JM, Salghetti SE, Tansey WP (2008). Modulation of RNA polymerase II subunit composition by ubiquitylation. Proc Natl Acad Sci USA 105, 19649–19654.
Delorme-Axford E, Guimaraes RS, Reggiori F, Klionsky DJ (2015). The yeast Saccharomyces cerevisiae: an overview of methods to study autophagy progression. Methods 75, 3–12.
Enenkel C (2014). Nuclear transport of yeast proteasomes. Biomolecules 4, 940–955.
Fehlker M, Wendler P, Lehmann A, Enenkel C (2003). Blm3 is part of nascent proteasomes and is involved in a late stage of nuclear proteasome assembly. EMBO Rep 4, 959–963.
Finley D, Ulrich HD, Sommer T, Kaiser P (2012). The ubiquitin-proteasome system of Saccharomyces cerevisiae. Genetics 192, 319–360.
Galluzzi L, Baehrecke EH, Ballabio A, Boya P, Bravo-San Pedro JM, Cecconi F, Choi AM, Chu CT, Codogno P, Colombo MI, *et al*. (2017). Molecular definitions of autophagy and related processes. EMBO J 36, 1811–1836.
Gandin V, Masvidal L, Hulea L, Gravel SP, Cargnello M, McLaughlan S, Cai Y, Balanathan P, Morita M, Rajakumar A, *et al*. (2016). nanoCAGE reveals 5′ UTR features that define specific modes of translation of functionally related MTOR-sensitive mRNAs. Genome Res 26, 636–648.
Ganesan V, Willis SD, Chang KT, Beluch S, Cooper KF, Strich R (2019). Cyclin C directly stimulates Drp1 GTP affinity to mediate stress-induced mitochondrial hyperfission. Mol Biol Cell 30, 302–311.
Givvimani S, Munjal C, Tyagi N, Sen U, Metreveli N, Tyagi SC (2012). Mitochondrial division/mitophagy inhibitor (Mdivi) ameliorates pressure overload induced heart failure. PLoS One 7, e32388.
Gnanasundram SV, Kos M (2015). Fast protein-depletion system utilizing tetracycline repressible promoter and N-end rule in yeast. Mol Biol Cell 26, 762–768.
Gomes LC, Di Benedetto G, Scorrano L (2011). During autophagy mitochondria elongate, are spared from degradation and sustain cell viability. Nat Cell Biol 13, 589–598.
Gomes LC, Scorrano L (2013). Mitochondrial morphology in mitophagy and macroautophagy. Biochim Biophys Acta 1833, 205–212.
Gray JV, Petsko GA, Johnston GC, Ringe D, Singer RA, Werner-Washburne M (2004). "Sleeping beauty": quiescence in Saccharomyces cerevisiae. Microbiol Mol Biol Rev 68, 187–206.
Gross A, Katz SG (2017). Non-apoptotic functions of BCL-2 family proteins. Cell Death Differ 24, 1348–1358.
Hartmann-Petersen R, Seeger M, Gordon C (2003). Transferring substrates to the 26S proteasome. Trends Biochem Sci 28, 26–31.
Hiraishi H, Okada M, Ohtsu I, Takagi H (2009). A functional analysis of the yeast ubiquitin ligase Rsp5: the involvement of the ubiquitin-conjugating enzyme Ubc4 and poly-ubiquitination in ethanol-induced down-regulation of targeted proteins. Biosci Biotechnol Biochem 73, 2268–2273.
Holstege FC, Jennings EG, Wyrick JJ, Lee TI, Hengartner CJ, Green MR, Golub TR, Lander ES, Young RA (1998). Dissecting the regulatory circuitry of a eukaryotic genome. Cell 95, 717–728.
Horie C, Suzuki H, Sakaguchi M, Mihara K (2003). Targeting and assembly of mitochondrial tail-anchored protein Tom5 to the TOM complex depend on a signal distinct from that of tail-anchored proteins dispersed in the membrane. J Biol Chem 278, 41462–41471.
Huibregtse JM, Yang JC, Beaudenon SL (1997). The large subunit of RNA polymerase II is a substrate of the Rsp5 ubiquitin-protein ligase. Proc Natl Acad Sci USA 94, 3656–3661.
Ichimura Y, Kirisako T, Takao T, Satomi Y, Shimonishi Y, Ishihara N, Mizushima N, Tanida I, Kominami E, Ohsumi M, *et al*. (2000). A ubiquitin-like system mediates protein lipidation. Nature 408, 488–492.
Jantti J, Lahdenranta J, Olkkonen VM, Soderlund H, Keranen S (1999). SEM1, a homologue of the split hand/split foot malformation candidate gene Dss1, regulates exocytosis and pseudohyphal differentiation in yeast. Proc Natl Acad Sci USA 96, 909–914.
Jezek J, Chang KT, Joshi AM, Strich R (2019a). Mitochondrial translocation of cyclin C stimulates intrinsic apoptosis through Bax recruitment. EMBO Rep 20, e47425.
Jezek J, Smethurst DGJ, Stieg DC, Kiss ZAC, Hanley SE, Ganesan V, Chang KT, Cooper KF, Strich R (2019b). Cyclin C: The story of a non-cycling cyclin. Biology (Basel) 8, doi.10.3390/biology8010003.
Jezek J, Wang K, Yan R, Di Cristofano A, Cooper KF, Strich R (2019c). Synergistic repression of thyroid hyperplasia by cyclin C and Pten. J Cell Sci.
Jin C, Strich R, Cooper KF (2014a). Slt2p phosphorylation induces cyclin C nuclear-to-cytoplasmic translocation in response to oxidative stress. Mol Biol Cell 25, 1396–1407.
Jin M, He D, Backues SK, Freeberg MA, Liu X, Kim JK, Klionsky DJ (2014b). Transcriptional regulation by Pho23 modulates the frequency of autophagosome formation. Curr Biol 24, 1314–1322.
Jin C, Kim SK, Willis SD, Cooper KF (2015). The MAPKKKs Ste11 and Bck1 jointly transduce the high oxidative stress signal through the cell wall integrity MAP kinase pathway. Microb Cell 2, 329–342.
Kadosh D, Struhl K (1997). Repression by Ume6 involves recruitment of a complex containing Sin3 corepressor and Rpd3 histone deacetylase to target promoters. Cell 89, 365–371.
Karren MA, Coonrod EM, Anderson TK, Shaw JM (2005). The role of Fis1p-Mdv1p interactions in mitochondrial fission complex assembly. J Cell Biol 171, 291–301.
Kasahara A, Scorrano L (2014). Mitochondria: from cell death executioners to regulators of cell differentiation. Trends Cell Biolo 24, 761–770.
Khakhina S, Cooper KF, Strich R (2014). Med13p prevents mitochondrial fission and programmed cell death in yeast through nuclear retention of cyclin C. Mol Biol Cell 25, 2807–2816.
Kirisako T, Baba M, Ishihara N, Miyazawa K, Ohsumi M, Yoshimori T, Noda T, Ohsumi Y (1999). Formation process of autophagosome is traced with Apg8/Aut7p in yeast. J Cell Biol 147, 435–446.
Klosinska MM, Crutchfield CA, Bradley PH, Rabinowitz JD, Broach JR (2011). Yeast cells can access distinct quiescent states. Genes Dev 25, 336–349.
Krasley E, Cooper KF, Mallory MJ, Dunbrack R, Strich R (2006). Regulation of the oxidative stress response through Slt2p-dependent destruction of cyclin C in Saccharomyces cerevisiae. Genetics 172, 1477–1486.
Krause SA, Gray JV (2002). The protein kinase C pathway is required for viability in quiescence in Saccharomyces cerevisiae. Curr Biol 12, 588–593.
Kwolek-Mirek M, Zadrag-Tecza R (2014). Comparison of methods used for assessing the viability and vitality of yeast cells. FEMS Yeast Res 14, 1068–1079.
Lander GC, Estrin E, Matyskiela ME, Bashore C, Nogales E, Martin A (2012). Complete subunit architecture of the proteasome regulatory particle. Nature 482, 186–191.
Lee Y, Lee HY, Hanna RA, Gustafsson AB (2011). Mitochondrial autophagy by Bnip3 involves Drp1-mediated mitochondrial fission and recruitment of Parkin in cardiac myocytes. Am J Physiol Heart Circ Physiol 301, H1924–H1931.
Lehmann A, Janek K, Braun B, Kloetzel PM, Enenkel C (2002). 20 S proteasomes are imported as precursor complexes into the nucleus of yeast. J Mol Biol 317, 401–413.
Levin DE (2005). Cell wall integrity signaling in Saccharomyces cerevisiae. Microbiol Mol Biol Rev 69, 262–291.
Li N, Fassl A, Chick J, Inuzuka H, Li X, Mansour MR, Liu L, Wang H, King B, Shaik S, *et al*. (2014). Cyclin C is a haploinsufficient tumour suppressor. Nat Cell Biol 16, 1080–1091.
Li X, Kusmierczyk AR, Wong P, Emili A, Hochstrasser M (2007). beta-Subunit appendages promote 20S proteasome assembly by overcoming an Ump1-dependent checkpoint. EMBO J 26, 2339–2349.
Liu YJ, McIntyre RL, Janssens GE, Houtkooper RH (2020). Mitochondrial fission and fusion: A dynamic role in aging and potential target for age-related disease. Mech Ageing Dev 186, 111212.
Loewith R, Hall MN (2011). Target of rapamycin (TOR) in nutrient signaling and growth control. Genetics 189, 1177–1201.
Loos B, du Toit A, Hofmeyr JH (2014). Defining and measuring autophagosome flux-concept and reality. Autophagy 10, 2087–2096.
Lorente J, Velandia C, Leal JA, Garcia-Mayea Y, Lyakhovich A, Kondoh H, ME LL (2018). The interplay between autophagy and tumorigenesis: exploiting autophagy as a means of anticancer therapy. Biol Rev Camb Philos Soc 93, 152–165.
Ludovico P, Rodrigues F, Almeida A, Silva MT, Barrientos A, Corte-Real M (2002). Cytochrome c release and mitochondria involvement in programmed cell death induced by acetic acid in Saccharomyces cerevisiae. Mol Biol Cell 13, 2598–2606.
Madeo F, Frohlich E, Ligr M, Grey M, Sigrist SJ, Wolf DH, Frohlich KU (1999). Oxygen stress: a regulator of apoptosis in yeast. J Cell Biol 145, 757–767.
Malinovska L, Kroschwald S, Munder MC, Richter D, Alberti S (2012). Molecular chaperones and stress-inducible protein-sorting factors coordinate the spatiotemporal distribution of protein aggregates. Mol Biol Cell 23, 3041–3056.

Mallory MJ, Strich R (2003). Ume1p represses meiotic gene transcription in *Saccharomyces cerevisiae* through interaction with the histone deacetylase Rpd3p. J Biol Chem 278, 44727–44734.
Mendl N, Occhipinti A, Muller M, Wild P, Dikic I, Reichert AS (2011). Mitophagy in yeast is independent of mitochondrial fission and requires the stress response gene WHI2. J Cell Sci 124, 1339–1350.
Mishra P, Chan DC (2016). Metabolic regulation of mitochondrial dynamics. J Cell Biol 212, 379–387.
Morita M, Prudent J, Basu K, Goyon V, Katsumura S, Hulea L, Pearl D, Siddiqui N, Strack S, McGuirk S, *et al.* (2017). mTOR controls mitochondrial dynamics and cell survival via MTFP1. Mol Cell 67, 922–935.e925.
Müller M, Kötter P, Behrendt C, Walter E, Scheckhuber CQ, Entian K-D, Reichert AS (2015). Synthetic quantitative array technology identifies the Ubp3-Bre5 deubiquitinase complex as a negative regulator of mitophagy. Cell Rep 10, 1215–1225.
Nair U, Thumm M, Klionsky DJ, Krick R (2011). GFP-Atg8 protease protection as a tool to monitor autophagosome biogenesis. Autophagy 7, 1546–1550.
Narasimhan J, Staschke KA, Wek RC (2004). Dimerization is required for activation of eIF2 kinase Gcn2 in response to diverse environmental stress conditions. J Biol Chem 279, 22820–22832.
Noda T (2008). Viability assays to monitor yeast autophagy. Methods Enzymol 451, 27–32.
Ong SB, Subrayan S, Lim SY, Yellon DM, Davidson SM, Hausenloy DJ (2010). Inhibiting mitochondrial fission protects the heart against ischemia/reperfusion injury. Circulation 121, 2012–2022.
Paraskevopoulos K, Kriegenburg F, Tatham MH, Rosner HI, Medina B, Larsen IB, Brandstrup R, Hardwick KG, Hay RT, Kragelund BB, *et al.* (2014). Dss1 is a 26S proteasome ubiquitin receptor. Mol Cell 56, 453–461.
Pereira C, Camougrand N, Manon S, Sousa M, Corte-Real M (2007). ADP/ATP carrier is required for mitochondrial outer membrane permeabilization and cytochrome c release in yeast apoptosis. Mol Microbiol 66, 571–582. Epub 2007 Sep 2006.
Perez-Perez ME, Zaffagnini M, Marchand CH, Crespo JL, Lemaire SD (2014). The yeast autophagy protease Atg4 is regulated by thioredoxin. Autophagy 10, 1953–1964.
Pickart CM (2001). Mechanisms underlying ubiquitination. Annu Rev Biochem 70, 503–533.
Rambold AS, Kostelecky B, Elia N, Lippincott-Schwartz J (2011a). Tubular network formation protects mitochondria from autophagosomal degradation during nutrient starvation. Proc Natl Acad Sci USA 108, 10190–10195.
Rambold AS, Kostelecky B, Lippincott-Schwartz J (2011b). Together we are stronger: fusion protects mitochondria from autophagosomal degradation. Autophagy 7, 1568–1569.
Ramos PC, Hockendorff J, Johnson ES, Varshavsky A, Dohmen RJ (1998). Ump1p is required for proper maturation of the 20S proteasome and becomes its substrate upon completion of the assembly. Cell 92, 489–499.
Reinke A, Chen JC, Aronova S, Powers T (2006). Caffeine targets TOR complex I and provides evidence for a regulatory link between the FRB and kinase domains of Tor1p. J Biol Chem 281, 31616–31626.
Ronne H, Rothstein R (1988). Mitotic sectored colonies: evidence of heteroduplex DNA formation during direct repeat recombination. Proc Natl Acad Sci USA 85, 2696–2700.
Rosenzweig R, Bronner V, Zhang D, Fushman D, Glickman MH (2012). Rpn1 and Rpn2 coordinate ubiquitin processing factors at proteasome. J Biol Chem 287, 14659–14671.
Rubinsztein DC, Marino G, Kroemer G (2011). Autophagy and aging. Cell 146, 682–695.
Saeki Y (2017). Ubiquitin recognition by the proteasome. J Biochem 161, 113–124.
Schauber C, Chen L, Tongaonkar P, Vega I, Lambertson D, Potts W, Madura K (1998). Rad23 links DNA repair to the ubiquitin/proteasome pathway. Nature 391, 715–718.
Shamas-Din A, Kale J, Leber B, Andrews DW (2013). Mechanisms of action of Bcl-2 family proteins. Cold Spring Harb Perspect Biol 5, a008714.
Shi Y, Chen X, Elsasser S, Stocks BB, Tian G, Lee BH, Shi Y, Zhang N, de Poot SA, Tuebing F, *et al.* (2016). Rpn1 provides adjacent receptor sites for substrate binding and deubiquitination by the proteasome. Science 351, doi.10.1126/science.aad9421.
Shpilka T, Weidberg H, Pietrokovski S, Elazar Z (2011). Atg8: an autophagy-related ubiquitin-like protein family. Genome Biol 12, 226.
Shpilka T, Welter E, Borovsky N, Amar N, Shimron F, Peleg Y, Elazar Z (2015). Fatty acid synthase is preferentially degraded by autophagy upon nitrogen starvation in yeast. Proc Natl Acad Sci USA 112, 1434–1439.
Srivastava S (2017). The mitochondrial basis of aging and age-related disorders. Genes (Basel) 8, doi.10.3390/genes8120398.
Stieg DC, Willis SD, Ganesan V, Ong KL, Scuorzo J, Song M, Grose J, Strich R, Cooper KF (2018). A complex molecular switch directs stress-induced cyclin C nuclear release through SCF(Grr1)-mediated degradation of Med13. Mol Biol Cell 29, 363–375.
Stieg DC, Chang KT, Cooper KF, Strich R (2019). Cyclin C regulated oxidative stress responsive transcriptome in *Mus musculus* embryonic fibroblasts. G3 9, 1901–1908.
Stoll KE, Brzovic PS, Davis TN, Klevit RE (2011). The essential Ubc4/Ubc5 function in yeast is HECT E3-dependent, and RING E3-dependent pathways require only monoubiquitin transfer by Ubc4. J Biol Chem 286, 15165–15170.
Strich R, Cooper K (2014). The dual role of cyclin C connects stress regulated gene expression to mitochondrial dynamics. Microbial Cell 1, 318–324.
Strich R, Slater MR, Esposito RE (1989). Identification of negative regulatory genes that govern the expression of early meiotic genes in yeast. Proc Natl Acad Sci USA 86, 10018–10022.
Strich R, Surosky RT, Steber C, Dubois E, Messenguy F, Esposito RE (1994). UME6 is a key regulator of nitrogen repression and meiotic development. Genes Dev 8, 796–810.
Sun N, Youle RJ, Finkel T (2016). The mitochondrial basis of aging. Mol Cell 61, 654–666.
Surosky RT, Strich R, Esposito RE (1994). The yeast *UME5* gene regulates the stability of meiotic mRNAs in response to glucose. Mol Cell Biol 14, 3446–3458.
Suzuki K, Kirisako T, Kamada Y, Mizushima N, Noda T, Ohsumi Y (2001). The pre-autophagosomal structure organized by concerted functions of APG genes is essential for autophagosome formation. EMBO J 20, 5971–5981.
Tait SW, Green DR (2013). Mitochondrial regulation of cell death. Cold Spring Harb Perspect Biol 5, doi.10.1101/cshperspect.a008706.
Takeshige K, Baba M, Tsuboi S, Noda T, Ohsumi Y (1992). Autophagy in yeast demonstrated with proteinase-deficient mutants and conditions for its induction. J Cell Biol 119, 301–311.
Tate JJ, Cooper TG (2013). Five conditions commonly used to down-regulate tor complex 1 generate different physiological situations exhibiting distinct requirements and outcomes. J Biol Chem 288, 27243–27262.
Tieu Q, Nunnari J (2000). Mdv1p is a WD repeat protein that interacts with the dynamin-related GTPase, Dnm1p, to trigger mitochondrial division. J Cell Biol 151, 353–366.
Tomko RJ Jr, Hochstrasser M (2014). The intrinsically disordered Sem1 protein functions as a molecular tether during proteasome lid biogenesis. Mol Cell 53, 433–443.
Torggler R, Papinski D, Kraft C (2017). Assays to Monitor Autophagy in Saccharomyces cerevisiae. Cells 6, doi.10.3390/cells6030023.
Tsuchiya H, Ohtake F, Arai N, Kaiho A, Yasuda S, Tanaka K, Saeki Y (2017). In vivo ubiquitin linkage-type analysis reveals that the Cdc48-Rad23/Dsk2 axis contributes to K48-linked chain specificity of the proteasome. Mol Cell 66, 488–502.e487.
Uekusa Y, Okawa K, Yagi-Utsumi M, Serve O, Nakagawa Y, Mizushima T, Yagi H, Saeki Y, Tanaka K, Kato K (2014). Backbone (1)H, (1)(3)C and (1)(5)N assignments of yeast Ump1, an intrinsically disordered protein that functions as a proteasome assembly chaperone. Biomol NMR Assign 8, 383–386.
van de Peppel J, Kettelarij N, van Bakel H, Kockelkorn TT, van Leenen D, Holstege FC (2005). Mediator expression profiling epistasis reveals a signal transduction pathway with antagonistic submodules and highly specific downstream targets. Mol Cell 19, 511–522.
Van Den Hazel HB, Kielland-Brandt MC, Winther JR (1996). Review: biosynthesis and function of yeast vacuolar proteases. Yeast 12, 1–16.
Varshavsky A (1992). The N-end rule. Cell 69, 725–735.
Verma R, Oania R, Graumann J, Deshaies RJ (2004). Multiubiquitin chain receptors define a layer of substrate selectivity in the ubiquitin-proteasome system. Cell 118, 99–110.
Vidal M, Strich R, Esposito RE, Gaber RF (1991). RPD1 (SIN3/UME4) is required for maximal activation and repression of diverse yeast genes. Mol Cell Biol 11, 6306–6316.

Vlahakis A, Lopez Muniozguren N, Powers T (2017). Stress-response transcription factors Msn2 and Msn4 couple TORC2-Ypk1 signaling and mitochondrial respiration to ATG8 gene expression and autophagy. Autophagy 13, 1804–1812.
Waite KA, De-La Mota-Peynado A, Vontz G, Roelofs J (2016). Starvation induces proteasome autophagy with different pathways for core and regulatory particles. J Biol Chem 291, 3239–3253.
Wang K, Yan R, Cooper KF, Strich R (2015). Cyclin C mediates stress-induced mitochondrial fission and apoptosis. Mol Biol Cell 26, 1030–1043.
Wang G, Yang J, Huibregtse JM (1999). Functional domains of the Rsp5 ubiquitin-protein ligase. Mol Cell Biol 19, 342–352.
Wang X, Yen J, Kaiser P, Huang L (2010). Regulation of the 26S proteasome complex during oxidative stress. Sci Signal 3, ra88.
Willis SD, Stieg DC, Ong KL, Shah R, Strich AK, Grose JH, Cooper KF (2018). Snf1 cooperates with the CWI MAPK pathway to mediate the degradation of Med13 following oxidative stress. Microbial Cell 5, 357–370.
Wissing S, Ludovico P, Herker E, Buttner S, Engelhardt SM, Decker T, Link A, Proksch A, Rodrigues F, Corte-Real M, *et al*. (2004). An AIF orthologue regulates apoptosis in yeast. J Cell Biol 166, 969–974.
Xie Z, Nair U, Klionsky DJ (2008). Atg8 controls phagophore expansion during autophagosome formation. Mol Biol Cell 19, 3290–3298.
Yukawa M, Yo K, Hasegawa H, Ueno M, Tsuchiya E (2009). The Rpd3/HDAC complex is present at the URS1 cis-element with hyperacetylated histone H3. Biosci Biotechnol Biochem 73, 378–384.
Zhang D, Chen T, Ziv I, Rosenzweig R, Matiuhin Y, Bronner V, Glickman MH, Fushman D (2009). Together, Rpn10 and Dsk2 can serve as a polyubiquitin chain-length sensor. Mol Cell 36, 1018–1033.
Zhu J, Deng S, Lu P, Bu W, Li T, Yu L, Xie Z (2016). The Ccl1-Kin28 kinase complex regulates autophagy under nitrogen starvation. J Cell Sci 129, 135–144.